

Entanglement harvesting from conformal vacuums between two Unruh-DeWitt detectors moving along null paths

Subhajit Barman,^{1,*} Dipankar Barman,^{1,†} and Bibhas Ranjan Majhi^{1,‡}

¹*Department of Physics, Indian Institute of Technology Guwahati, Guwahati 781039, Assam, India*

(Dated: September 23, 2022)

It is well-known that the $(1+1)$ dimensional Schwarzschild and spatially flat FLRW spacetimes are conformally flat. This work examines entanglement harvesting from the conformal field vacuums in these spacetimes between two Unruh-DeWitt detectors, moving along outgoing null trajectories. In $(1+1)$ dimensional Schwarzschild spacetime, we considered the Boulware and Unruh vacuums for our investigations. In this analysis, one observes that while entanglement harvesting is possible in $(1+1)$ dimensional Schwarzschild and $(1+3)$ dimensional de Sitter spacetimes, it is not possible in the $(1+1)$ dimensional de Sitter background for the same set of parameters when the detectors move along the same outgoing null trajectory. The qualitative results from the Boulware and the Unruh vacuums are alike. Furthermore, we observed that the concurrence depends on the distance d between the two null paths of the detectors periodically, and depending on the parameter values, there could be entanglement harvesting shadow points or regions. We also observe that the mutual information does not depend on d in $(1+1)$ dimensional Schwarzschild and de Sitter spacetimes but periodically depends on it in $(1+3)$ dimensional de Sitter background. We also provide elucidation on the origin of the harvested entanglement.

PACS numbers: 04.62.+v, 04.60.Pp

I. INTRODUCTION

The fascinating phenomenon of quantum entanglement has garnered significant interest in the scenarios of relativistic particles in flat and curved spacetimes [1–18]. Studying the dynamics of entangled particles in flat and curved spacetimes [9, 19–21] has presented many enthralling perspectives. Another interesting facet is the possibility of entanglement extraction [1, 6, 22–28] from the quantum field into atoms or other suitable systems interacting with the field, which is known as entanglement harvesting. The prospect of utilizing this harvested entanglement in quantum information-related purposes [29–31] to solidify experimental verification of many theoretical predictions has made the harvesting a desirable arena to venture further.

Reznik solidified the possibility of harvesting entanglement from the vacuum of the background quantum field in [1, 25] where he recognized entanglement extraction in a system of two anti-parallelly accelerated two-level atomic detectors. Reznik’s work signifies the role of the quantum field vacuum in entanglement extraction as one observes entanglement harvesting between two causally disconnected accelerated detectors with no possibility of classical correlation. His works and the subsequent works [7, 32–41] usually deal with a system composed of two detectors that interact with the background field and are in an initial uncorrelated state. One can perceive any entanglement harvested between the two detectors by checking

whether the partial transposition of the final system reduced density matrix has negative eigenvalues [42, 43]. We mention that one realizes this reduced density matrix as the system’s final density matrix with the field degrees of freedom traced out. This formulation was further improved in [44–49], where the authors considered proper time ordering into the picture. It resulted in the introduction of the Feynman propagator rather than the Wightman function in some places of the estimated eigenvalues. We mention that the entanglement harvesting condition and the measure of the harvested entanglement depends on the background geometry [32–34, 49–51], boundary conditions [15, 50, 52], the two detectors’ trajectories [6, 49, 53], etc.

Recently, entanglement harvesting in black hole spacetimes [26, 47, 49, 54] has gained much interest. In this context, which vacuum to choose in these spacetimes to formulate quantum field theory and obtain the Green’s functions corresponding to observers in different trajectories has a general notion [49]. Namely, in an $(1+1)$ dimensional Schwarzschild background, these are the *Boulware*, *Unruh*, and *Hartle-Hawking vacuums* [49]. They denote conformal vacuums corresponding to different coordinate choices in the background spacetime, as all $(1+1)$ dimensional spacetimes are conformally flat [55, 56]. We mention that the spatially flat *Friedman-Lemaître-Robertson-Walker* (FLRW) metric is also conformally flat. One should also note that nontrivial findings for entanglement harvesting is closely related to semi-classical particle creation. However, in a $(1+1)$ dimensional Schwarzschild background, a static observer does not see the Boulware vacuum to be particle creating. Likewise, with static detectors, one obtains entanglement harvesting related observations from the Boulware vacuum that are similar to the flat spacetime [49]. Furthermore, in [57], it was

*Electronic address: subhajit.b@iitg.ac.in

†Electronic address: dipankar1998@iitg.ac.in

‡Electronic address: bibhas.majhi@iitg.ac.in

shown that a radially in-falling detector in a time-like trajectory observes the Boulware vacuum to be thermal. These freely-falling detectors also keep nontrivial entanglement harvesting profiles from the Boulware vacuum, as was pointed out in [49]. Subsequently, in [58, 59], one also observes the thermal nature of the Boulware vacuum and that of the conformal vacuum in the FLRW spacetime, with detectors infalling in null-like trajectories. These facts motivated us to study entanglement-related phenomena with detectors in null paths in the $(1+1)$ dimensional Schwarzschild and FLRW spacetimes. In particular, we shall investigate the entanglement harvesting from the above-mentioned conformal vacuums in these backgrounds. This consideration of null trajectories for detectors in black hole spacetimes is interesting from the point of view that it may shed light on the entanglement harvested between light-like particles emitted from astrophysical bodies along null paths. In this regard, we mention that these are situations related to the Hawking effect, as originally, Hawking, in his pioneering work [60] elucidated the black hole evaporation in terms of field modes in ingoing and outgoing null trajectories. Thus our consideration of entanglement harvesting along null trajectories may open up directions to provide new insights towards the understanding of the black hole information loss paradox and also remains relevant from the cosmological point of view.

As we have already stated, in this work, we study the entanglement harvesting conditions with Unruh-DeWitt detectors in null trajectories in the background of $(1+1)$ -dimensional Schwarzschild black holes and the FLRW spacetime. The Unruh-DeWitt detectors conceptualized to understand the Unruh effect [61–63], are point-like two-level hypothetical detectors. In particular, we have considered estimating the entanglement harvesting condition in the de Sitter era of the FLRW universe. We also mention that we obtain the entanglement harvesting condition for each specific field mode frequency. We observe that entanglement harvesting is indeed possible from the conformal vacuums in $(1+1)$ dimensional Schwarzschild, $(1+1)$ and $(1+3)$ dimensional FLRW spacetimes with two detectors in outgoing null paths. In all these cases except the $(1+1)$ dimensional de Sitter spacetime, the concurrence, which measures the harvested entanglement, peaks at a particular field mode frequency when the detectors move along the same path. Furthermore, the interesting phenomenon is that this concurrence is, in all these cases, periodically dependent on the distance d ($\neq 0$) between different outgoing null paths of the two detectors. In particular, we observe that in $(1+1)$ dimensional Schwarzschild and $(1+3)$ dimensional de Sitter backgrounds, there are periodic zero entanglement harvesting regions and points in the distance d corresponding to low and high values of the field frequency respectively. In contrast, for $(1+1)$ dimensional de Sitter spacetime, one only perceives zero entanglement harvesting regions. Thus providing the notion of the so-called entanglement shadow points and shadow regions [26, 54],

from where one cannot harvest entanglement. However, unlike [26, 54] where the entanglement shadow region appears near the black hole event horizon, in our case, these regions are periodic in the distance d . On the other hand, we observe that the mutual information in $(1+1)$ dimensional Schwarzschild and de Sitter spacetimes are independent of this distance d between the null paths of the two detectors. However, in $(1+3)$ dimensional de Sitter spacetime, the mutual information is dependent on d . We also observe that it is periodic with the distance d between different outgoing null paths of the two detectors.

We organize this paper in the following way. In Sec. II we start with a brief overview of the model set-up for entanglement harvesting with two two-level point-like atomic detectors interacting with the background massless real scalar field through monopole couplings. This section elucidates the entanglement harvesting condition, the measure of the harvested entanglement (the concurrence), and the total correlation (the mutual information). In Sec. III we illuminate the importance of conformal vacuum in curved spacetimes to formulate quantum field theory and briefly discuss the construction of these vacuums in FLRW and $(1+1)$ dimensional Schwarzschild spacetimes. Subsequently, in Sec. V we consider a massless conformally invariant scalar field in these spacetimes and construct the necessary Green's functions for observers in null trajectories. In Sec. VI we study the entanglement harvesting condition from the conformal vacuum in the spacetimes as mentioned earlier and also study the entanglement measure concurrence. Furthermore, in Sec. VII we provide a discussion on the origin of the harvested entanglement. In particular, we try to understand how much of the harvested entanglement is from the background field state, considered truly harvested, and how much is due to communication between the detectors. In the following section VIII we investigate the mutual information in the considered spacetimes. We conclude this work in Sec. IX with a discussion of our findings.

II. MODEL SET-UP

In this section, we will briefly discuss the model set up for entanglement harvesting, emphasizing the necessary notations and symbols of the different system parameters. This model was introduced initially in [44–46], which keeps into consideration the necessary time ordering in the construction of the Green's functions.

In this model set-up, one considers two point-like two-level Unruh-DeWitt detectors, each carried by a distinct observer. One of these observers is Alice denoted by A , and another one is Bob denoted by B . We denote the detector states as $|E_n^j\rangle$, with the symbols delineating the n^{th} state of j^{th} detector, i.e., we have $j = A, B$ and $n = 0, 1$. We also consider these states to be

non degenerate so that $E_1^j \neq E_0^j$, and the difference $\Delta E^j = E_1^j - E_0^j > 0$ signifies the transition frequency. Furthermore, we consider a massless, minimally coupled real scalar field $\Phi(X)$ interacting with these detectors through monopole couplings $m^j(\tau_j)$. One can express the corresponding interaction action as

$$S_{int} = \int_{-\infty}^{\infty} \left[c_A \kappa_A(\tau_A) m^A(\tau_A) \Phi(X_A(\tau_A)) d\tau_A + c_B \kappa_B(\tau_B) m^B(\tau_B) \Phi(X_B(\tau_B)) d\tau_B \right], \quad (1)$$

where, c_j , $\kappa_j(\tau_j)$, and τ_j respectively denote the cou-

plings between the individual detectors and the scalar field, the switching functions, and the individual detector proper times. We consider the initial detector field state in the asymptotic past to be $|in\rangle = |0\rangle|E_0^A\rangle|E_0^B\rangle$, where $|0\rangle$ denotes the field's ground state. Then the final detector field state in asymptotic future will be $|out\rangle = T\{e^{iS_{int}}|in\rangle\}$, where T signifies time ordering. One can get the explicit expression of this final state by treating the coupling constants c_j perturbatively. In this way and by tracing out the final field degrees of freedoms one obtains the final detector density matrix in the basis of $\{|E_1^A\rangle|E_1^B\rangle, |E_1^A\rangle|E_0^B\rangle, |E_0^A\rangle|E_1^B\rangle, |E_0^A\rangle|E_0^B\rangle\}$ as

$$\rho_{AB} = \begin{bmatrix} 0 & 0 & 0 & c_A c_B \varepsilon \\ 0 & c_A^2 P_A & c_A c_B P_{AB} & c_A^2 W_A^{(N)} + c_A c_B W_A^{(S)} \\ 0 & c_A c_B P_{AB}^* & c_B^2 P_B & c_B^2 W_B^{(N)} + c_A c_B W_B^{(S)} \\ c_A c_B \varepsilon^* & c_A^2 W_A^{(N)*} + c_A c_B W_A^{(S)*} & c_B^2 W_B^{(N)*} + c_A c_B W_B^{(S)*} & 1 - (c_A^2 P_A + c_B^2 P_B) \end{bmatrix} + \mathcal{O}(c^4), \quad (2)$$

where, P_j , ε , $W_j^{(N)}$, and $W_j^{(S)}$ are explicitly expressed as

$$P_j = |\langle E_1^j | m_j(0) | E_0^j \rangle|^2 \mathcal{I}_j$$

$$\varepsilon = \langle E_1^B | m_B(0) | E_0^B \rangle \langle E_1^A | m_A(0) | E_0^A \rangle \mathcal{I}_\varepsilon$$

$$P_{AB} = \langle E_1^A | m_A(0) | E_0^A \rangle \langle E_1^B | m_B(0) | E_0^B \rangle^\dagger \mathcal{I}_{AB}$$

$$W_j^{(N)} = \langle E_1^j | m_j(0) | E_0^j \rangle \left[\left(\langle E_1^j | m_j(0) | E_1^j \rangle - \langle E_0^j | m_j(0) | E_0^j \rangle \right) \mathcal{I}_{j,1}^{(N)} - i \langle E_0^j | m_j(0) | E_0^j \rangle \mathcal{I}_{j,2}^{(N)} \right]$$

$$W_j^{(S)} = -i \langle E_1^j | m_j(0) | E_0^j \rangle \langle E_0^{j'} | m_{j'}(0) | E_0^{j'} \rangle \mathcal{I}_j^{(S)}, \quad (3)$$

where $j' \neq j$ and the quantities \mathcal{I} 's are given by

$$\mathcal{I}_j = \int_{-\infty}^{\infty} d\tau_j' \int_{-\infty}^{\infty} d\tau_j e^{-i\Delta E^j(\tau_j' - \tau_j)} G_W(X_j', X_j),$$

$$\mathcal{I}_\varepsilon = -i \int_{-\infty}^{\infty} d\tau_B' \int_{-\infty}^{\infty} d\tau_A e^{i(\Delta E^B \tau_B' + \Delta E^A \tau_A)} G_F(X_B', X_A),$$

$$\mathcal{I}_{AB} = \int_{-\infty}^{\infty} d\tau_B' \int_{-\infty}^{\infty} d\tau_A e^{i(\Delta E^A \tau_A - \Delta E^B \tau_B')} G_W(X_B', X_A),$$

$$\mathcal{I}_{j,1}^{(N)} = \int_{-\infty}^{\infty} d\tau_j' \int_{-\infty}^{\infty} d\tau_j e^{i\Delta E^j \tau_j} \theta(\tau_j' - \tau_j) G_W(X_j', X_j),$$

$$\mathcal{I}_{j,2}^{(N)} = \int_{-\infty}^{\infty} d\tau_j' \int_{-\infty}^{\infty} d\tau_j e^{i\Delta E^j \tau_j} G_R(X_j, X_j'),$$

$$\mathcal{I}_j^{(S)} = \int_{-\infty}^{\infty} d\tau_j' \int_{-\infty}^{\infty} d\tau_j e^{i\Delta E^j \tau_j} G_R(X_j, X_j'). \quad (4)$$

Here we have considered $\kappa_j(\tau_j) = 1$, i.e., the detectors are eternally interacting with the field. The expressions of the quantities $G_W(X_j, X_{j'})$, $G_F(X_j, X_{j'})$, and $G_R(X_j, X_{j'})$; which respectively denote the positive frequency Wightman function with $X_j > X_{j'}$, the Feynman propagator, and the retarded Green's function; are [44]

$$\begin{aligned} G_W(X_j, X_{j'}) &\equiv \langle 0_M | \Phi(X_j) \Phi(X_{j'}) | 0_M \rangle, \\ G_F(X_j, X_{j'}) &\equiv -i \langle 0_M | T \{ \Phi(X_j) \Phi(X_{j'}) \} | 0_M \rangle, \\ G_R(X_j, X_{j'}) &\equiv i \theta(t - t') \langle 0_M | [\Phi(X_{j'}), \Phi(X_j)] | 0_M \rangle. \end{aligned} \quad (5)$$

We refer the readers to [44] for a complete analysis.

From the general study [42, 43] of bipartite systems, it is observed that one must have a negative eigenvalue of the partial transposition of the reduced detector density matrix for entanglement harvesting. Here, with the reduced density matrix (2) this condition results in

$$P_A P_B < |\varepsilon|^2. \quad (6)$$

Moreover, in terms of the integrals (4) this condition (6) takes the form [44, 46]

$$\mathcal{I}_A \mathcal{I}_B < |\mathcal{I}_\varepsilon|^2. \quad (7)$$

We mention that the Feynman propagator and the Wightman functions are related among themselves [44] as $iG_F(X_j, X_{j'}) = G_W(X_j, X_{j'}) + iG_R(X_{j'}, X_j) = G_W(X_j, X_{j'}) + \theta(T' - T)\{G_W(X_{j'}, X_j) - G_W(X_j, X_{j'})\}$, which can be used to further simplify the expression of the integral \mathcal{I}_ε of (4) as

$$\begin{aligned} \mathcal{I}_\varepsilon = & - \int_{-\infty}^{\infty} d\tau_B \int_{-\infty}^{\infty} d\tau_A e^{i(\Delta E^B \tau_B + \Delta E^A \tau_A)} \\ & \times \left[G_W(X_B, X_A) + \theta(T_A - T_B) \right. \\ & \left. \times \{G_W(X_A, X_B) - G_W(X_B, X_A)\} \right]. \end{aligned} \quad (8)$$

This particular expression is advantageous because all of the integrals \mathcal{I}_A , \mathcal{I}_B and \mathcal{I}_ε , imperative for the verification of the entanglement harvesting condition (7), are now expressed in terms of the Wightman functions. Furthermore writing the \mathcal{I}_ε in this form also enables one to identify the separate contributions with or without the considered time ordering. Note that condition (7) is constructed at the order c^2 in perturbation series. Later on our whole analysis will be done at this order.

After the condition for entanglement harvesting (7) is met, one is prompted to quantify its measures. The common entanglement measures are negativity and concurrence [64–67]. Negativity signifies the upper bound of the distillable entanglement, and one obtains it from the sum of all negative eigenvalues of the partial transpose of ρ_{AB} . Concurrence $\mathcal{C}(\rho_{AB})$ is another convenient entanglement measure [20, 44, 46], which enables one to find the entanglement of formation [44, 46, 68–70]. In the two qubits system, the concurrence is given by [44]

$$\begin{aligned} \mathcal{C}(\rho_{AB}) = & \max \left[0, 2c^2 \left(|\varepsilon| - \sqrt{P_A P_B} \right) + \mathcal{O}(c^4) \right] \\ \approx & \max \left[0, 2c^2 |\langle E_1^B | m_B(0) | E_0^B \rangle| |\langle E_1^A | m_A(0) | E_0^A \rangle| \right. \\ & \left. \times \left(|\mathcal{I}_\varepsilon| - \sqrt{\mathcal{I}_A \mathcal{I}_B} \right) \right], \end{aligned} \quad (9)$$

where, we have assumed $c_A = c_B = c$, i.e., both detectors have equal couplings with the scalar field. Now the quantities $|\langle E_1^j | m_j(0) | E_0^j \rangle|$ are obtained from the detectors' internal structure; the spacetime and background scalar fields do not contribute in them. Then to understand the effects of the trajectories and the spacetime in the harvested entanglement, we shall only study the relevant quantity

$$\mathcal{C}_\mathcal{I} = \left(|\mathcal{I}_\varepsilon| - \sqrt{\mathcal{I}_A \mathcal{I}_B} \right) \quad (10)$$

with the intention of studying the concurrence. Note in the symmetric case $\mathcal{I}_A = \mathcal{I}_B$, this quantity becomes $\mathcal{C}_\mathcal{I} = (|\mathcal{I}_\varepsilon| - \mathcal{I}_j)$, see [44, 46].

Another measure of correlation is mutual information \mathcal{M} , which signifies the total of classical and quantum

correlations, defined as

$$\mathcal{M}(\rho_{AB}) \equiv S(\rho_A) + S(\rho_B) - S(\rho_{AB}), \quad (11)$$

where, $\rho_A \equiv \text{Tr}_B(\rho_{AB})$ and $\rho_B \equiv \text{Tr}_A(\rho_{AB})$ are the reduced density matrices corresponding to the detectors A and B , and $S(\rho) \equiv -\text{Tr}(\rho \ln \rho)$ signifies the von Neumann entropy corresponding to the density matrix ρ . With the density matrix (2), and considering equal couplings between the two detectors and field, one can express the mutual information [71] of (11) as

$$\begin{aligned} \mathcal{M}(\rho_{AB}) = & c^2 [P_+ \ln P_+ + P_- \ln P_- - P_A \ln P_A \\ & - P_B \ln P_B] + \mathcal{O}(c^4), \end{aligned} \quad (12)$$

where, the quantities P_\pm are given by

$$P_\pm = \frac{1}{2} \left[P_A + P_B \pm \sqrt{(P_A - P_B)^2 + 4|P_{AB}|^2} \right]. \quad (13)$$

In a system, if the mutual information is non-zero but the concurrence vanishes, then the correlation is considered classical. Consequently, we shall look into both concurrence and mutual information to understand the nature of the correlation between the two detectors.

III. CONFORMAL VACUUM FOR TWO DIMENSIONAL SCHWARZSCHILD BLACK HOLE AND FLRW UNIVERSE

In this section, we are going to discuss the conformal vacuum associated with a $(1+1)$ dimensional Schwarzschild and *Friedman-Lemaître-Robertson-Walker* (FLRW) spacetime. Although the concept is elaborated in literature [55, 56] in great detail, here we shall provide a brief outline of the essential elements necessary for our study. Introducing a conformally invariant field in conformally flat spacetime allows one to realize flat-space-like quantum field theory in a curved background without moving to its asymptotic regions. The metric tensor corresponding to a conformally flat spacetime can be expressed as

$$g_{\mu\nu}(x) = \Omega^2 \eta_{\mu\nu}(x), \quad (14)$$

where Ω^2 is the conformal factor, and $\eta_{\mu\nu}(x)$ denotes the metric tensor in a Minkowski spacetime. In a conformally flat spacetime it is necessary to consider a massless ($m = 0$) scalar field $\Phi(x)$ to obtain a conformally invariant wave equation. In particular, this wave equation is expressed as

$$(\square - \xi R) \Phi(x) = 0, \quad (15)$$

where the operator \square in the background spacetime is given by $\square \Phi = (\sqrt{-g})^{-1/2} \partial_\mu [\sqrt{-g} g^{\mu\nu} \partial_\nu \Phi]$, R represents the Ricci scalar, and ξ the conformal coupling. In an n -dimensional spacetime this conformal coupling is of the form $\xi = (n-2)/4(n-1)$. Therefore, ξ vanishes in $(1+1)$ -dimensional spacetime and $\xi = 1/6$

for $(1+3)$ -dimensions. It is to be noted that with a further decomposition of the conformally invariant field $\Phi = \Omega^{(2-n)/2} \bar{\Phi}$, the above wave equation reduces to that of the flat spacetime, $\eta^{\mu\nu} \partial_\nu \partial_\mu (\bar{\Phi}) = 0$. Then one could readily find out the mode solutions \bar{u}_k of the field $\bar{\Phi}$, which are plane wave like. In terms of these mode functions one may express the scalar field $\Phi(x)$ as

$$\Phi(x) = \Omega^{(2-n)/2}(x) \sum_k [\hat{a}_k \bar{u}_k(x) + \hat{a}_k^\dagger \bar{u}_k^*(x)] . \quad (16)$$

Here the annihilation operator \hat{a}_k annihilates the conformal vacuum $|0\rangle$, i.e., $\hat{a}_k|0\rangle = 0$. This brief summary highlights the advantages of considering a conformally coupled scalar field in a conformally flat spacetime to observe the effects of quantum field theory. It should be noted that all $(1+1)$ dimensional spacetimes and the spatially flat FLRW spacetime are conformally flat. In our subsequent analysis we shall briefly discuss the conformal nature of Schwarzschild and FLRW spacetimes.

A. Two dimensional Schwarzschild spacetime

In this part, we are going to elucidate on the Schwarzschild spacetime briefly. In particular, we shall concentrate on the $(1+1)$ dimensional representation of it. There are a few necessary reasons behind considering the $(1+1)$ dimensional representation. In our context, the most important reason is that all $(1+1)$ dimensional spacetimes are conformally flat, as we have previously mentioned. Then one can effortlessly utilize quantum field theory in this background. For semi-classical particle production, one usually needs the understanding of wave modes in ingoing and outgoing null paths in a black hole background. This picture is efficiently understandable in an $(1+1)$ dimensional representation of a generally higher-dimensional black hole spacetime to produce the thermal behavior of the Hawking effect. This outcome also becomes relevant in our scenario, as Entanglement harvesting is closely related to particle production. The $(1+1)$ dimensional representation of the Schwarzschild solution is considered to understand the entanglement harvesting conditions with static and free-falling detectors in literature [49], which will also help us compare our results.

In fact, the $(1+1)$ dimensional Schwarzschild black hole can be considered as the solution of a two dimensional Einstein-Dilaton theory [56, 72] which is a dimensionally reduced form of higher dimensional usual Einstein's theory of gravity. In particular, in $(1+1)$ dimensions the line-element in Schwarzschild background using the Schwarzschild coordinates (t_s, r) is given by

$$ds^2 = -\left(1 - \frac{r_H}{r}\right) dt_s^2 + \left(1 - \frac{r_H}{r}\right)^{-1} dr^2 , \quad (17)$$

where, r_H represents the Schwarzschild radius. It is observed that in terms of the tortoise coordinate r_* , defined

from

$$dr_* = \frac{dr}{1 - r_H/r} , \quad (18)$$

the $(1+1)$ dimensional Schwarzschild metric becomes

$$ds^2 = \left(1 - \frac{r_H}{r}\right) [-dt_s^2 + dr_*^2] . \quad (19)$$

The expression of this metric is analogous to the prescription of (14) with $\Omega^2 = (1 - r_H/r)$, which ensures that the $(1+1)$ dimensional Schwarzschild black hole spacetime is conformally flat. One can easily obtain the scalar field decomposition like (16) in this spacetime, with the wave modes now expressed in terms of t_s and r_* . In particular, the related conformal vacuum is known as the Boulware vacuum.

We mention that the conformal metric of (19) can also be represented in terms of the null coordinates $u = t_s - r_*$ and $v = t_s + r_*$, thus the Boulware modes are eligible to be represented in terms of these null coordinates. These null coordinates are related to the Kruskal coordinates as $V = 2r_H e^{v/2r_H}$ and $U = -2r_H e^{-u/2r_H}$. One may move to these Kruskal coordinates also and find the metric of Eq. (19) again to be conformally flat, but with different conformal factors. We mention that considering different sets of these coordinates one obtains different conformal vacuums corresponding to the Schwarzschild black hole spacetime. Specifically with u and v the vacuum is Boulware, with U and v the vacuum is Unruh, and U and V the vacuum is Hartle-Hawking [49, 73].

A static observer in a Schwarzschild black hole spacetime does not observe the Boulware vacuum to be filled with particles. However, a freely in-falling observer perceives the Boulware vacuum to be thermal, as was pointed out by recent studies [57]. On the other hand, entanglement related observations are highly connected to the scenarios of particle creation in a curved spacetime [49]. Therefore, we shall consider these types of relevant paths, which can observe particles in these vacua, for the observation of entanglement harvesting.

B. The FLRW spacetime

After briefly elucidating on the static black hole spacetime we now proceed to the *Friedman-Lemaître-Robertson-Walker* (FLRW) spacetime, which is an exact solution of the Einstein's field equations with positive cosmological constant. The FLRW metric was formulated to represent our universe and indicates spatial homogeneity, isotropy, and expansion. In $(1+1)$ -dimensional FLRW spacetime the line element is given by

$$ds^2 = -dt^2 + a^2(t) dx^2 , \quad (20)$$

where $a(t)$ denotes the scale factor, which is different in different eras of the universe. In particular, in this work

we shall consider the de Sitter era, where one can analytically pursue the calculations. In de Sitter era the scale factor is $a(t) = e^{t/\alpha_d}$, which describes the early expansion of the homogeneous, isotropic universe. In terms of the conformal time η , related to the coordinate time t through $d\eta = dt/a(t)$, expressed in de Sitter background

$$\eta = -\alpha_d e^{-t/\alpha_d}, \quad (21)$$

the line element becomes

$$ds^2 = a^2(\eta)(-d\eta^2 + dx^2). \quad (22)$$

Like the (1+1) dimensional Schwarzschild spacetime here also one can observe that the background spacetime becomes conformally flat with $\Omega = a(\eta)$, and one can easily find out the scalar field decomposition like (16) with respect to the coordinates η and x .

On the other hand, in (1+3)-dimensional FLRW spacetime the line element is given by

$$\begin{aligned} ds^2 &= -dt^2 + a^2(t)|d\vec{x}|^2 \\ &= a^2(\eta)(-d\eta^2 + |d\vec{x}|^2). \end{aligned} \quad (23)$$

Here also the spacetime is conformally flat and one is eligible to decompose a conformally coupled scalar field in terms of plane wave modes. It is to be noted that, in both the (1+1) and (1+3) dimensional de Sitter spacetimes the conformal vacuums for observers with coordinates (η, \vec{x}) are perceived to be particle creating with respect to a co-moving observer with coordinates (t, \vec{x}) .

In [58], it is shown that an observer in a null like trajectory also observes the conformal vacuum particle generating. We have already stated semi-classical particle creation is closely related to non-trivial findings in the entanglement harvesting conditions. In our subsequent studies we shall be discussing about the null paths in these spacetimes which are related to particle creation. Furthermore, we shall investigate the entanglement harvesting conditions in these scenarios.

IV. NULL PATHS RELATED TO PARTICLE CREATION FROM THE CONFORMAL VACUUM

Here we discuss a class of trajectories, specifically the null paths, from which an observer perceives the conformal vacuum to be particle creating. First, in a (1+1) dimensional black hole Schwarzschild spacetime Eq. (19) signifies that a radially moving object is following an outgoing null path if $u = t_s - r_*$ is constant along its trajectory. On the other hand, it is ingoing when $v = t_s + r_*$ is constant. These two coordinates are often referred to as the retarded and advanced time coordinates or the outgoing and ingoing null coordinates. In terms of the Eddington-Finkelstein (EF) coordinates (t, r) , with $t + r = t_s + r_*$ the metric (19) transforms to

$$ds^2 = -\left(1 - \frac{r_H}{r}\right)dt^2 + \frac{2r_H}{r}dtdr + \left(1 + \frac{r_H}{r}\right)dr^2. \quad (24)$$

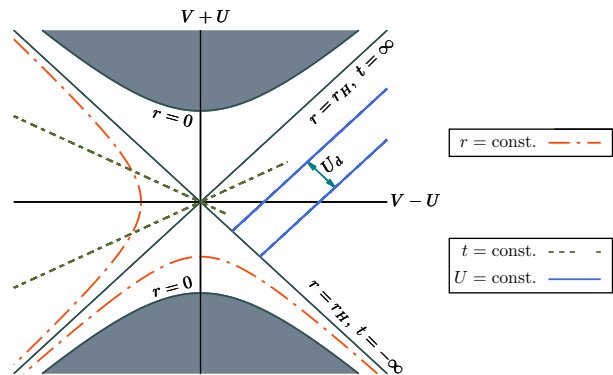


FIG. 1: Schematic representation of two detectors in outgoing null paths depicted in a Kruskal diagram. In Eddington-Finkelstein coordinates the two detectors are separated as $u_A - u_b = d$, while in Kruskal coordinates they are separated as $U_d = U_B - U_A = 2r_H(1 - e^{-d/2r_H})$, where $U_j = -2r_H e^{-u_j/2r_H}$.

With these EF coordinates one can find out an outgoing null trajectory by making $ds^2 = 0$ in (24) and considering the positive solution of dr/dt , see [59], as

$$\frac{dt}{dr} = \frac{r/r_H + 1}{r/r_H - 1}, \quad (25)$$

which gives the path to be

$$t = r + 2r_H \ln \left[\frac{r}{r_H} - 1 \right] + d. \quad (26)$$

Here d is a constant parameter arriving as an integration constant from Eq. (25). In Fig. 1 we have provided a Kruskal diagram depicting the null rays in a (1+1) dimensional Schwarzschild black hole spacetime, and in this figure one also notices that d distinguishes different outgoing null paths. We mention that, utilizing quantum field theory one can perceive particle production in conformal Boulware vacuum with respect to observers, moving along these null paths [58, 59].

On the other hand, the outgoing and ingoing null coordinates in a general de Sitter background is given by $u = \eta - |\vec{x}|$ and $v = \eta + |\vec{x}|$. One can simply understand that these expressions in (1+1) dimensions become $u = \eta - x$ and $v = \eta + x$. With respect to the coordinate time t an observer along these null paths perceives the conformal vacuum particle generating. The scenarios of particle creation in curved spacetimes also influences the entanglement related observations. Therefore, we are going to consider these null trajectories in the Schwarzschild and FLRW spacetimes to understand the entanglement harvesting conditions from the relevant conformal vacuums.

V. GREEN'S FUNCTION CORRESPONDING TO OUTGOING NULL DETECTORS

From Eq. (7) and (4) of Sec. II we have seen that it is imperative to construct the Green's functions for a considered trajectory in a background spacetime to understand the entanglement harvesting conditions in this scenario. In this section, we will construct these necessary Green's functions along the null paths in the previously considered Schwarzschild and FLRW spacetimes. In this regard, we mention that rather than considering these Green's functions in their position space representations, we will take them in their momentum space representations. This consideration allows one to evaluate detector transition probabilities corresponding to a specific field mode frequency even with linear field-detector interaction in $(1+1)$ dimensions. With this particular consideration, we also observed that one could circumvent the issues related to the infrared cutoff inherent to the $(1+1)$ dimensional massless scalar field theory.

A. Schwarzschild background

1. Boulware vacuum

The positive frequency Boulware modes in terms of the null coordinates u and v are given by $e^{-i\omega u}$ and $e^{-i\omega v}$. One can then decompose a massless minimally coupled scalar field Φ in terms of these Boulware modes and suitably choosing the sets of creation and annihilation operators $\{\hat{a}_k^{B\dagger}, \hat{a}_k^B\}$ and $\{\hat{b}_k^{B\dagger}, \hat{b}_k^B\}$ as [74]

$$\Phi = \int_0^\infty \frac{d\omega_k}{\sqrt{4\pi\omega_k}} \left[\hat{a}_k^B e^{-i\omega_k u} + \hat{a}_k^{B\dagger} e^{i\omega_k u} + \hat{b}_k^B e^{-i\omega_k v} + \hat{b}_k^{B\dagger} e^{i\omega_k v} \right]. \quad (27)$$

The ladder operators satisfy the commutation relation $[\hat{a}_k^B, \hat{a}_{k'}^{B\dagger}] = \delta_{k,k'}$ and $[\hat{b}_k^B, \hat{b}_{k'}^{B\dagger}] = \delta_{k,k'}$, where all other choices in the commutator vanishes. Also the Boulware vacuum $|0\rangle_B$ is now defined by the one annihilated by these annihilation operators $\hat{a}_k^B |0\rangle_B = 0 = \hat{b}_k^B |0\rangle_B$. Then using the above field decomposition one can get the positive frequency Wightman function with respect to the Boulware vacuum to be given by

$$\begin{aligned} G_B^+(X_j, X_l) &= {}_B\langle 0 | \Phi(X_j) \Phi(X_l) | 0 \rangle_B \\ &= \int_0^\infty \frac{d\omega_k}{4\pi\omega_k} [e^{-i\omega_k(u_j - u_l)} + e^{-i\omega_k(v_j - v_l)}], \end{aligned} \quad (28)$$

where the subscript j and l correspond to the events X_j and X_l respectively.

Now we shall be considering one detector, say detector A with a non zero d , and detector B with $d = 0$. Then we shall be using $t_A = r_A + 2r_H \ln[r_A/r_H - 1] + d$ and $t_B = r_B + 2r_H \ln[r_B/r_H - 1]$. Using these EF coordinates, for

two detectors following outgoing null trajectories (26), one has the quantities

$$\begin{aligned} v'_j - v_l &= t'_{s_j} + r'_{*j} - (t_{s_l} + r_{*l}) \\ &= 2(r'_j - r_l) + 2r_H \ln \left[\frac{r'_j - r_H}{r_l - r_H} \right] \\ &\quad + d(\delta_{jA} \delta_{lB} - \delta_{jB} \delta_{lA}), \end{aligned} \quad (29)$$

and

$$\begin{aligned} u'_j - u_l &= t'_{s_j} - r'_{*j} - (t_{s_l} - r_{*l}) \\ &= d(\delta_{jA} \delta_{lB} - \delta_{jB} \delta_{lA}), \end{aligned} \quad (30)$$

where j and l can represent either detector A or B , with δ_{jl} denoting the *Kronecker delta* defined as

$$\begin{aligned} \delta_{jl} &= 0, \quad \text{if } j \neq l \\ &= 1, \quad \text{if } j = l. \end{aligned} \quad (31)$$

Substitution of (29) and (30) in (28) provides us the required Green's function G_B^+ corresponding to the Boulware vacuum with respect to our observers.

2. Unruh vacuum

To discuss about the Unruh modes and the corresponding Unruh vacuum one needs an understanding of the Kruskal coordinates $V = 2r_H e^{v/2r_H}$, and $U = -2r_H e^{-u/2r_H}$. Then the positive frequency Unruh modes in terms of the null coordinates v and U are given by $e^{-i\omega U}$ and $e^{-i\omega v}$. In terms of these Unruh modes a massless minimally coupled scalar field Φ is decomposed, choosing the sets of creation and annihilation operators $\{\hat{a}_k^{U\dagger}, \hat{a}_k^U\}$ and $\{\hat{b}_k^{U\dagger}, \hat{b}_k^U\}$, as

$$\Phi = \int_0^\infty \frac{d\omega_k}{\sqrt{4\pi\omega_k}} \left[\hat{a}_k^U e^{-i\omega_k v} + \hat{a}_k^{U\dagger} e^{i\omega_k v} + \hat{b}_k^U e^{-i\omega_k U} + \hat{b}_k^{U\dagger} e^{i\omega_k U} \right]. \quad (32)$$

The ladder operators satisfy the commutation relation $[\hat{a}_k^U, \hat{a}_{k'}^{U\dagger}] = \delta_{k,k'}$ and $[\hat{b}_k^U, \hat{b}_{k'}^{U\dagger}] = \delta_{k,k'}$, where all other choices in the commutator vanishes. Also the Unruh vacuum $|0\rangle_U$ is now defined by the one annihilated by these annihilation operators $\hat{a}_k^U |0\rangle_U = 0 = \hat{b}_k^U |0\rangle_U$. Then using the above field decomposition one can get the positive frequency Wightman function with respect to the Unruh vacuum to be given by

$$\begin{aligned} G_U^+(X_j, X_l) &= {}_U\langle 0 | \Phi(X_j) \Phi(X_l) | 0 \rangle_U \\ &= \int_0^\infty \frac{d\omega_k}{4\pi\omega_k} [e^{-i\omega_k(v_j - v_l)} + e^{-i\omega_k(U_j - U_l)}], \end{aligned} \quad (33)$$

where the subscript j and l correspond to the events X_j and X_l respectively. To write this in terms of our chosen trajectories we need to use the following transformation

relations. Using the EF coordinates, for two detectors in outgoing null trajectories (26), one has these relations

$$\begin{aligned} v'_j - v_l &= t'_{s_j} + r'_{*j} - (t_{s_l} + r_{*l}) \\ &= 2(r'_j - r_l) + 2r_H \ln \left[\frac{r'_j - r_H}{r_l - r_H} \right] \\ &\quad + d(\delta_{jA} \delta_{lB} - \delta_{jB} \delta_{lA}), \end{aligned} \quad (34)$$

and

$$\begin{aligned} U'_j - U_l &= -2r_H e^{-\frac{u'_j}{2r_H}} - (-2r_H e^{-\frac{u_l}{2r_H}}) \\ &= 2r_H \left(1 - e^{-\frac{d}{2r_H}} \right) (\delta_{jA} \delta_{lB} - \delta_{jB} \delta_{lA}). \end{aligned} \quad (35)$$

B. de Sitter spacetime

1. (1+1)-dimensions

Let us consider a massless minimally coupled scalar field Φ in the (1+1) dimensional de Sitter background denoted by (22). In particular, the equation of motion for the field Φ suggests field mode solutions of the form $u_\nu = e^{\mp i\omega_k(\eta \mp x)}$. Let us construct like the Schwarzschild case the outgoing and ingoing null coordinates $u = \eta - x$ and $v = \eta + x$. Then with a suitable set of creation and annihilation operators and with these mode functions one can decompose the scalar field as

$$\begin{aligned} \Phi &= \int_0^\infty \frac{d\omega_k}{\sqrt{4\pi\omega_k}} \left[\hat{a}_k^D e^{-i\omega_k u} + \hat{a}_k^{D\dagger} e^{i\omega_k u} \right. \\ &\quad \left. + \hat{b}_k^D e^{-i\omega_k v} + \hat{b}_k^{D\dagger} e^{i\omega_k v} \right], \end{aligned} \quad (36)$$

where the annihilation operators \hat{a}_k^D and \hat{b}_k^D annihilate the de Sitter vacuum $|0\rangle_D$. Then with the help of this field decomposition one can express the Green's function as

$$\begin{aligned} G_D^+(X_j, X_l) &= {}_D\langle 0 | \Phi(X_j) \Phi(X_l) | 0 \rangle_D \\ &= \int_0^\infty \frac{d\omega_k}{4\pi\omega_k} [e^{-i\omega_k(u_j - u_l)} + e^{-i\omega_k(v_j - v_l)}]. \end{aligned} \quad (37)$$

We also mention that along outgoing null trajectory $u = \eta - x$ is constant and along an ingoing null trajectory $v = \eta + x$ is constant. We consider our two observers Alice and Bob moving in outgoing null trajectories, and for Alice $\eta = x + d$ while for Bob $\eta = x$. With the help of Kronecker delta δ_{jl} one can collectively express these differences as

$$\begin{aligned} u_j - u_l &= d(\delta_{jA} \delta_{lB} - \delta_{jB} \delta_{lA}) \\ v_j - v_l &= 2\alpha_d (e^{-t_l/\alpha_d} - e^{-t_j/\alpha_d}) \\ &\quad - d(\delta_{jA} \delta_{lB} - \delta_{jB} \delta_{lA}), \end{aligned} \quad (38)$$

where, j and l can take values of either A or B . Substituting (38) in (37) we will find our required G_D^+ with respect to the outgoing trajectory.

2. (1+3)-dimensions

In (1+3) dimensional de Sitter spacetime also the conformal factor is $\Omega = a(\eta)$ like (1+1) dimensions. However, the difference in the spacetime dimensionality results in a factor of $a(\eta)^{(2-4)/2}$ in the scalar field decomposition of (16). In particular, in a (1+3)-dimensional FLRW universe a conformally coupled scalar field Φ in can be decomposed into modes and ladder operators as,

$$\begin{aligned} \Phi &= \int \frac{d^3k}{\sqrt{(2\pi)^3 2\omega_k}} \frac{1}{a(\eta)} \left(e^{-i\omega_k \eta + i\vec{k} \cdot \vec{x}} \hat{b}_{\vec{k}, \omega_k} \right. \\ &\quad \left. + e^{i\omega_k \eta - i\vec{k} \cdot \vec{x}} \hat{b}_{\vec{k}, \omega_k}^\dagger \right). \end{aligned} \quad (39)$$

For simplicity, we choose the detectors to be outgoing along the x axis. Then along this path $\Delta y = 0 = \Delta z$, and only the k_x component from the factor $\vec{k} \cdot \vec{x}$ will survive in the Green's function evaluated with respect to the conformal vacuum. The Wightman functions for these outgoing null paths are given by

$$G_W(X_j, X_l) = \int \frac{d^3k}{(2\pi)^3 2\omega_k} \frac{e^{ik_x \Delta x_{jl} - i\omega_k \Delta \eta_{jl}}}{a(\eta_j) a(\eta_l)}. \quad (40)$$

For the case when the detectors are moving along the x axis, i.e., the motion of the detectors are actually confined to a one dimensional line, the outgoing null paths corresponding to Alice and Bob are again $\eta = x + d$ and $\eta = x$. One can use the information of these paths to obtain the appropriate Δx_{jl} and $\Delta \eta_{jl}$ in a straightforward manner. Then one can substitute these expressions in (40) to obtain the necessary Green's functions in the null trajectories.

VI. ENTANGLEMENT HARVESTING

A. Schwarzschild background

1. Boulware vacuum

As we have already discussed we are considering one detector, say detector A with a non zero d , and detector B with $d = 0$. First we shall use the expression of the Wightman function estimated in the Boulware vacuum from Eq. (28). With the coordinate transformations of Eq. (29) and (30) suitable to an observer in an outgoing null path in a Schwarzschild black hole spacetime, one can compute the necessary integrals of (7) to investigate the entanglement harvesting condition. In particular, one can find out the individual detector transition probabilities \mathcal{I}_j as

$$\begin{aligned} \mathcal{I}_j &= \int_{-\infty}^\infty dt'_j \int_{-\infty}^\infty dt_j e^{-i\Delta E^j(t'_j - t_j)} G_B^+(X'_j, X_j) \\ &= \int_0^\infty \frac{d\omega_k}{4\pi\omega_k} \mathcal{I}_{j\omega_k}. \end{aligned} \quad (41)$$

Here the integrals $\mathcal{I}_{j\omega_k}$ are represented as

$$\begin{aligned}\mathcal{I}_{j\omega_k} &= \int_{-\infty}^{\infty} dt'_j \int_{-\infty}^{\infty} dt_j e^{-i\Delta E^j(t'_j - t_j)} \\ &\quad \times [e^{-i\omega_k(u_{j'} - u_j)} + e^{-i\omega_k(v_{j'} - v_j)}] \\ &= \int_{-\infty}^{\infty} dt'_j \int_{-\infty}^{\infty} dt_j e^{-i\Delta E^j(t'_j - t_j)} \\ &\quad \times \left[1 + e^{-2i\omega_k(r_{j'} - r_j)} \left(\frac{r_{j'} - r_H}{r_j - r_H} \right)^{-2ir_H\omega_k} \right], \quad (42)\end{aligned}$$

where we have used the relations from Eq. (29) and (30). Here we mention that the integrations over the first additive unity provides multiplicative factors of the Dirac delta distributions $\delta(\Delta E^j)$, which makes the contribution of that part of the integration to vanish as the detector transition energy $\Delta E^j > 0$. Then we consider the expression of (25) for the realization of outgoing null paths in this calculation and the expression (42) transforms into

$$\begin{aligned}\mathcal{I}_{j\omega_k} &= \int_{r_H}^{\infty} dr_{j'} \frac{r_{j'} + r_H}{r_{j'} - r_H} \int_{r_H}^{\infty} dr_j \frac{r_j + r_H}{r_j - r_H} \\ &\quad \times e^{-i(\Delta E^j + 2\omega_k)(r_{j'} - r_j)} \left(\frac{r_{j'} - r_H}{r_j - r_H} \right)^{-2ir_H(\Delta E^j + \omega_k)} \quad (43)\end{aligned}$$

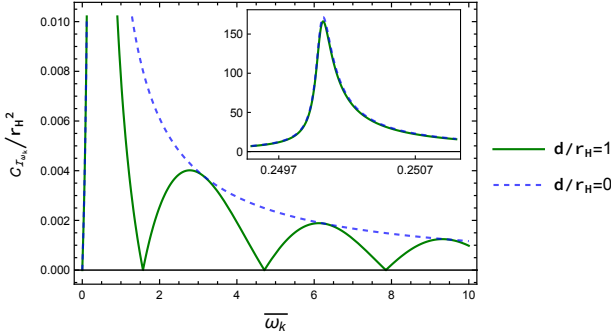


FIG. 2: The quantity $C_{\mathcal{I}_{\omega_k}}/r_H^2 = (|\mathcal{I}_{\varepsilon\omega_k}| - \mathcal{I}_{j\omega_k})/r_H^2$, signifying the concurrence, is plotted for two outgoing null detectors in a (1 + 1) dimensional Schwarzschild black hole spacetime with respect to the dimensionless frequency of the field $\bar{\omega}_k = r_H\omega_k$ for fixed detector transition energies $\Delta E^A = r_H\Delta E^A = 0.5$, $\Delta E^B = r_H\Delta E^B = 0.5$. The other parameter is fixed at $d/r_H = 0$ and $d/r_H = 1$.

Now one may consider a change of variables $y'_j = r_{j'}/r_H - 1$ and $y_j = r_j/r_H - 1$. Then this integral simplifies to

$$\mathcal{I}_{j\omega_k} = r_H^2 \left| \int_0^{\infty} dy_j \frac{y_j + 2}{y_j} \frac{e^{ir_H(\Delta E^j + 2\omega_k)y_j}}{y_j^{-2ir_H(\Delta E^j + \omega_k)}} \right|^2. \quad (44)$$

To evaluate this integral we introduce regulator of the form $y_j^\epsilon e^{-\epsilon y_j}$, where ϵ is a real positive parameter. Then the actual value of the integral is obtained by taking the

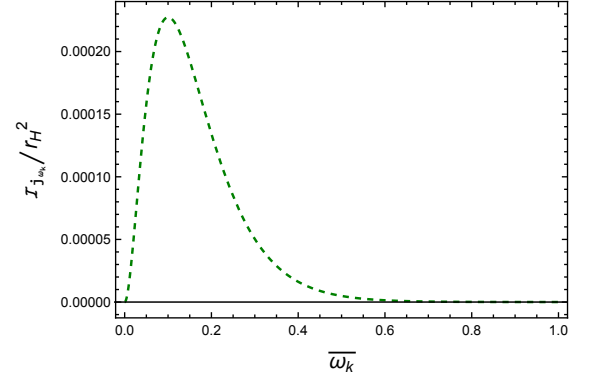


FIG. 3: The quantity $\mathcal{I}_{j\omega_k}/r_H^2$ is plotted for two outgoing null detectors in a (1 + 1) dimensional Schwarzschild black hole spacetime with respect to the frequency of the field $\bar{\omega}_k = r_H\omega_k$ for fixed detector transition energies $\Delta E^A = r_H\Delta E^A = 0.5$, $\Delta E^B = r_H\Delta E^B = 0.5$. One should note that $\mathcal{I}_{j\omega_k}$ is independent of the parameter d .

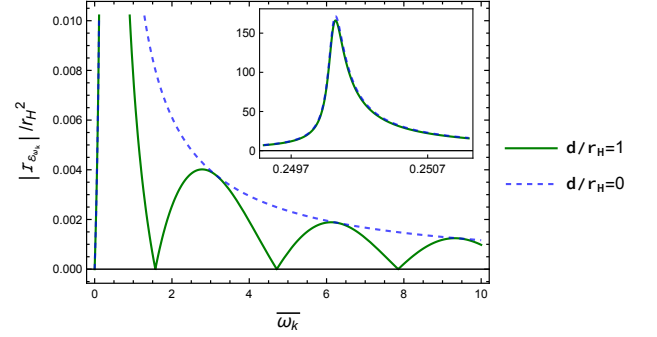


FIG. 4: The quantity $|\mathcal{I}_{\varepsilon\omega_k}|/r_H^2$ is plotted for two outgoing null detectors in a (1 + 1) dimensional Schwarzschild black hole spacetime with respect to the frequency of the field $\bar{\omega}_k = r_H\omega_k$ for fixed detector transition energies $\Delta E^A = r_H\Delta E^A = 0.5$, $\Delta E^B = r_H\Delta E^B = 0.5$, and fixed $d/r_H = 0$ and $d/r_H = 1$.

limit $\epsilon \rightarrow 0$ after evaluating the regulated integral as

$$\begin{aligned}\lim_{\epsilon \rightarrow 0} &\left[\int_0^{\infty} dy_j \frac{y_j + 2}{y_j} \frac{e^{ir_H(\Delta E^j + 2\omega_k)y_j - \epsilon y_j}}{y_j^{-2ir_H(\Delta E^j + \omega_k) - \epsilon}} \right] \\ &= e^{-\pi r_H(\Delta E^j + \omega_k)} \Gamma(2ir_H(\Delta E^j + \omega_k)) \\ &\quad \times \frac{2\omega_k(r_H(\Delta E^j + 2\omega_k))^{-2ir_H(\Delta E^j + \omega_k)}}{\Delta E^j + 2\omega_k}. \quad (45)\end{aligned}$$

The entire integral $\mathcal{I}_{j\omega_k}$ from (45) becomes

$$\begin{aligned}\mathcal{I}_{j\omega_k} &= \frac{4\pi r_H\omega_k^2}{(\Delta E^j + \omega_k)(\Delta E^j + 2\omega_k)^2} \\ &\quad \times \frac{1}{e^{4\pi r_H(\Delta E^j + \omega_k)} - 1}, \quad (46)\end{aligned}$$

where we have used the *Gamma function* identity $\Gamma(iz)\Gamma(-iz) = \pi/(z \sinh \pi z)$. This signifies a somewhat Planckian distribution with respect to the detector transition energy ΔE^j plus energy of each Boulware mode

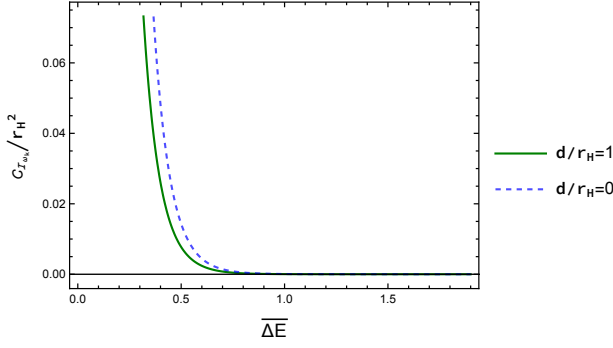


FIG. 5: The quantity $\mathcal{C}_{\mathcal{I}_{\omega_k}}/r_H^2$ is plotted for two outgoing null detectors in a (1 + 1) dimensional Schwarzschild black hole spacetime with respect to the dimensionless transition energy $\overline{\Delta E} = r_H \Delta E$ of the detectors, where $\Delta E = \Delta E^A = \Delta E^B$. The dimensionless field mode frequency is fixed at $\bar{\omega}_k = 1$ and the dimensionless distance between the null paths are $d/r_H = 0$ and $d/r_H = 1$.

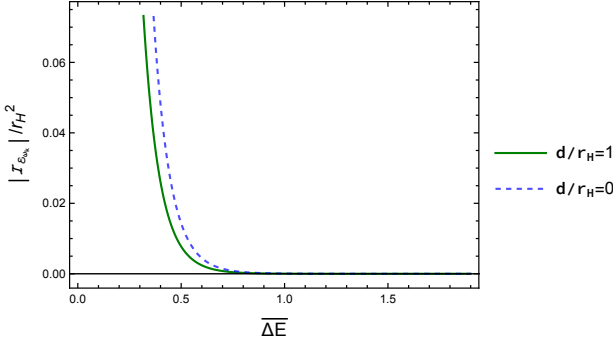


FIG. 6: The quantity $|\mathcal{I}_{\mathcal{E}_{\omega_k}}|/r_H^2$ is plotted for two outgoing null detectors in a (1+1) dimensional Schwarzschild black hole spacetime with respect to the dimensionless transition energy $\overline{\Delta E} = r_H \Delta E$ of the detectors, where $\Delta E = \Delta E^A = \Delta E^B$. The dimensionless field mode frequency is fixed at $\bar{\omega}_k = 1$ and the other fixed parameter are $d/r_H = 0$ and $d/r_H = 1$.

ω_k . On the other hand, for the evaluation of the integral $\mathcal{I}_{\mathcal{E}}$ we express it with the help of Eq. (8) as

$$\mathcal{I}_{\mathcal{E}} = -\mathcal{I}_{\mathcal{E}}^W - \mathcal{I}_{\mathcal{E}}^R, \quad (47)$$

where one has

$$\begin{aligned} \mathcal{I}_{\mathcal{E}}^W &= \int_{-\infty}^{\infty} d\tau_B \int_{-\infty}^{\infty} d\tau_A e^{i(\Delta E^B \tau_B + \Delta E^A \tau_A)} G_W(X_B, X_A) \\ &= \int_0^{\infty} \frac{d\omega_k}{4\pi\omega_k} \mathcal{I}_{\mathcal{E}_{\omega_k}}^W, \end{aligned} \quad (48)$$

and

$$\begin{aligned} \mathcal{I}_{\mathcal{E}}^R &= \int_{-\infty}^{\infty} d\tau_B \int_{-\infty}^{\infty} d\tau_A e^{i(\Delta E^B \tau_B + \Delta E^A \tau_A)} \theta(T_A - T_B) \\ &\quad \times [G_W(X_A, X_B) - G_W(X_B, X_A)] \\ &= \int_0^{\infty} \frac{d\omega_k}{4\pi\omega_k} \mathcal{I}_{\mathcal{E}_{\omega_k}}^R. \end{aligned} \quad (49)$$

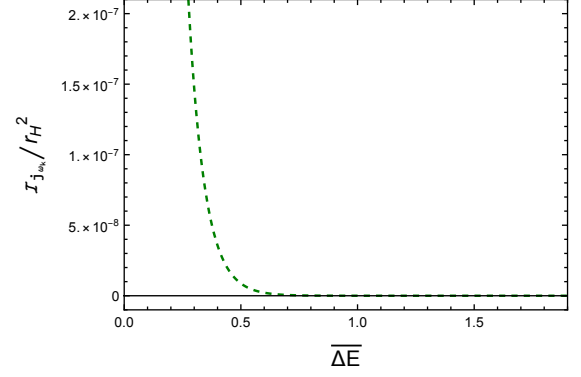


FIG. 7: The quantity $\mathcal{I}_{\mathcal{J}_{\omega_k}}/r_H^2$ is plotted for two outgoing null detectors in a (1 + 1) dimensional Schwarzschild black hole spacetime with respect to the dimensionless transition energy $\overline{\Delta E} = r_H \Delta E$ of the detectors, where $\Delta E = \Delta E^A = \Delta E^B$. The dimensionless field mode frequency is fixed at $\bar{\omega}_k = 1$. One should note that $\mathcal{I}_{\mathcal{J}_{\omega_k}}$ is independent of d .

One should note here the detector times τ_j are denoted by the EF times, i.e., $\tau_j = t_j$. On the other hand, the times T_j appearing in the Heaviside step function due to field decomposition are the Schwarzschild times t_{s_j} as the field decomposition has been done with respect to the Boulware modes. With the help of Eq. (29) and (30) one can express the integral $\mathcal{I}_{\mathcal{E}_{\omega_k}}^W$ as

$$\begin{aligned} \mathcal{I}_{\mathcal{E}_{\omega_k}}^W &= \int_{-\infty}^{\infty} dt_B \int_{-\infty}^{\infty} dt_A e^{i(\Delta E^B t_B + \Delta E^A t_A)} \\ &\quad \times [e^{-i\omega_k(u_B - u_A)} + e^{-i\omega_k(v_B - v_A)}] \\ &= \int_{-\infty}^{\infty} dt_B \int_{-\infty}^{\infty} dt_A e^{i(\Delta E^B t_B + \Delta E^A t_A)} \left[e^{i\omega_k d} \right. \\ &\quad \left. + e^{-i\omega_k(2r_B - 2r_A - d)} \left(\frac{r_B - r_H}{r_A - r_H} \right)^{-2ir_H\omega_k} \right]. \end{aligned} \quad (50)$$

Here also one can observe that the integration over the first quantity with $e^{i\omega_k d}$ as multiplicative factor will provide the multiplication of Dirac delta distributions $\delta(\Delta E^A)$ and $\delta(\Delta E^B)$. Therefore that part of the integral will vanish as the detector transition energy $\Delta E^j > 0$. Now like the evaluation of $\mathcal{I}_{\mathcal{J}_{\omega_k}}$ we utilize Eq. (26) and consider a change of variables $y_B = r_B/r_H - 1$ and $y_A = r_A/r_H - 1$, which will simplify the above integral to

$$\begin{aligned} \mathcal{I}_{\mathcal{E}_{\omega_k}}^W &= r_H^2 e^{id(\Delta E^A + \omega_k)} \\ &\quad \times \left[\int_0^{\infty} dy_B \frac{y_B + 2}{y_B} \frac{e^{ir_H(\Delta E^B - 2\omega_k)(y_B + 1)}}{y_B^{-2ir_H(\Delta E^B - \omega_k)}} \right. \\ &\quad \left. \times \int_0^{\infty} dy_A \frac{y_A + 2}{y_A} \frac{e^{ir_H(\Delta E^A + 2\omega_k)(y_A + 1)}}{y_A^{-2ir_H(\Delta E^A + \omega_k)}} \right]. \end{aligned} \quad (51)$$

The analytic expression of this integral (51) is given in Eq. (A1) of Appendix A1. On the other hand, one can

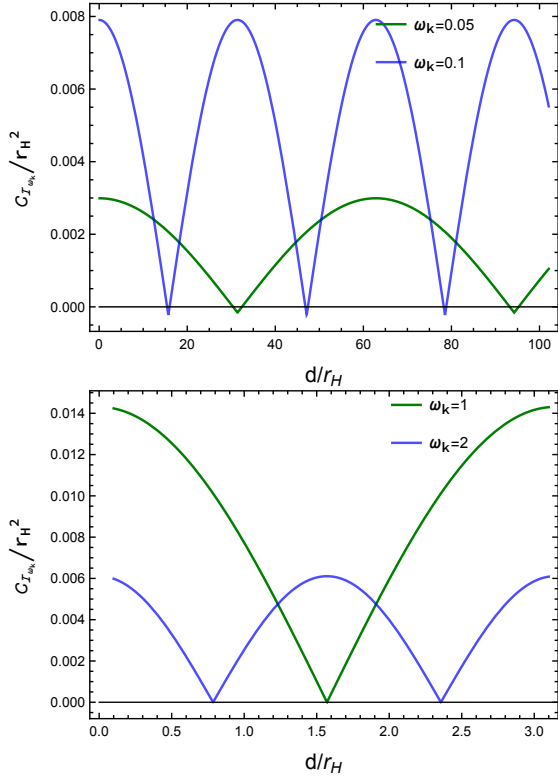


FIG. 8: The quantity $C_{I_{\omega_k}}/r_H^2$ is plotted for two outgoing null detectors in different parallel paths in a (1 + 1) dimensional Schwarzschild black hole spacetime with respect to the separation between the two paths d/r_H . The dimensionless frequency of the field are fixed at $\bar{\omega}_k = 0.05$ and $\bar{\omega}_k = 0.1$, respectively in the upper plot and shows entanglement shadow regions. Whereas in the lower plot, the dimensionless frequency of the field are fixed at $\bar{\omega}_k = 1$ and $\bar{\omega}_k = 2$, respectively and shows entanglement shadow points instead of the shadow regions. The detector transition energy is fixed at $\Delta E = 0.5$.

also express $\mathcal{I}_{\varepsilon\omega_k}^R$, which contains the contribution from a retarded Green's function, from Eq. (49) as

$$\begin{aligned} \mathcal{I}_{\varepsilon\omega_k}^R &= \int_{-\infty}^{\infty} dt_A \int_{-\infty}^{\infty} dt_B e^{i(\Delta E^B t_B + \Delta E^A t_A)} \theta(t_{s_A} - t_{s_B}) \\ &\times \left[e^{-i\omega_k(u_A - u_B)} + e^{-i\omega_k(v_A - v_B)} \right. \\ &\left. - e^{-i\omega_k(u_B - u_A)} - e^{-i\omega_k(v_B - v_A)} \right]. \end{aligned} \quad (52)$$

Here we mention that the Schwarzschild time t_s and the EF time t are related among themselves as $t + r = t_s + r_*$. Along an outgoing null trajectory (26) one readily gets $\theta(t_{s_A} - t_{s_B}) = \theta(r_{*A} + d - r_{*B})$. Then for any $d > 0$ as one takes $r_A > r_B$ the outcome $t_{s_A} > t_{s_B}$ is guaranteed, i.e., $\theta(r_A - r_B) \Rightarrow \theta(t_{s_A} - t_{s_B})$ for $d > 0$. In our analysis we have considered $d > 0$, transformed the coordinate t to r using relation (26), and utilized the $\theta(r_A - r_B)$ expression to change the limit of r_B to $[r_H, r_A]$ from $[r_H, \infty)$. Then

one can proceed to evaluate the integral of (52) as

$$\begin{aligned} \mathcal{I}_{\varepsilon\omega_k}^R &= \int_{r_H}^{\infty} dr_A \frac{r_A + r_H}{r_A - r_H} \int_{r_H}^{r_A} dr_B \frac{r_B + r_H}{r_B - r_H} \\ &\times e^{i\{\Delta E^B r_B + \Delta E^A (r_A + d)\}} \left(\frac{r_B}{r_H} - 1 \right)^{2ir_H \Delta E^B} \\ &\times \left(\frac{r_A}{r_H} - 1 \right)^{2ir_H \Delta E^A} \left[e^{-i\omega_k(2r_A + d - 2r_B)} \right. \\ &\times \left(\frac{r_A - r_H}{r_B - r_H} \right)^{-2ir_H \omega_k} - e^{-i\omega_k(2r_B - 2r_A - d)} \\ &\times \left(\frac{r_B - r_H}{r_A - r_H} \right)^{-2ir_H \omega_k} \left. - 2i \sin(\omega_k d) \right]. \end{aligned} \quad (53)$$

Here we notice that the contribution from the quantity $e^{-i\omega_k(u_A - u_B)} - e^{-i\omega_k(u_B - u_A)} = -2i \sin(\omega_k d)$ is independent of t_j . With the change of variables $y_B = r_B/r_H - 1$ and $y_A = r_A/r_H - 1$, the above integral simplifies to

$$\begin{aligned} \mathcal{I}_{\varepsilon\omega_k}^R &= r_H^2 \left[e^{-i\omega_k d} \int_0^{\infty} dy_A \frac{y_A + 2}{y_A} \frac{e^{ir_H(\Delta E^A - 2\omega_k)(y_A + 1)}}{y_A^{-2ir_H(\Delta E^A - \omega_k)}} \right. \\ &\int_0^{y_A} dy_B \frac{y_B + 2}{y_B} \frac{e^{ir_H(\Delta E^B + 2\omega_k)(y_B + 1)}}{y_B^{-2ir_H(\Delta E^B + \omega_k)}} \\ &- e^{i\omega_k d} \int_0^{\infty} dy_A \frac{y_A + 2}{y_A} \frac{e^{ir_H(\Delta E^A + 2\omega_k)(y_A + 1)}}{y_A^{-2ir_H(\Delta E^A + \omega_k)}} \\ &\int_0^{y_A} dy_B \frac{y_B + 2}{y_B} \frac{e^{ir_H(\Delta E^B - 2\omega_k)(y_B + 1)}}{y_B^{-2ir_H(\Delta E^B - \omega_k)}} \\ &- 2i \sin(\omega_k d) \int_0^{\infty} dy_A \frac{y_A + 2}{y_A} \frac{e^{ir_H \Delta E^A (y_A + 1)}}{y_A^{-2ir_H \Delta E^A}} \\ &\left. \int_0^{y_A} dy_B \frac{y_B + 2}{y_B} \frac{e^{ir_H \Delta E^B (y_B + 1)}}{y_B^{-2ir_H \Delta E^B}} \right] e^{i\Delta E^A d}. \end{aligned} \quad (54)$$

One may go through Appendix A1, Eq. (A2), for an analytical evaluation of this integral, which we have estimated introducing regulators. These regulators make the otherwise divergent integrals convergent. One gets the analytical expression of this integral in terms of the *Gamma functions* $\Gamma(x)$ and *Hypergeometric functions* ${}_2F_1(a, b; c; x)$. We also mention that the quantity with a multiplicative $2i \sin(\omega_k d)$ term here has negligible contribution compared to the other terms, see Appendix A2.

Like the concurrence defined in Eq. (10) one perceives that in the symmetric case the quantity $\mathcal{C}_{I_{\omega_k}} = (|\mathcal{I}_{\varepsilon\omega_k}| - \mathcal{I}_{j\omega_k})$ represents the concurrence corresponding to a specific field mode frequency ω_k , where $\mathcal{I}_{\varepsilon\omega_k} = \mathcal{I}_{\varepsilon\omega_k}^W + \mathcal{I}_{\varepsilon\omega_k}^R$. In Fig. 2 we have plotted the dimensionless quantity $\mathcal{C}_{I_{\omega_k}}/r_H^2$, which represents the concurrence, as a function of the dimensionless frequency $\bar{\omega}_k = r_H \omega_k$ for fixed $\Delta E^A = r_H \Delta E^A = 0.5$, $\Delta E^B = r_H \Delta E^B = 0.5$, and for $d/r_H = 0$ and $d/r_H = 1$ respectively. For $d/r_H = 0$ the entanglement harvesting takes a peak at a certain $\bar{\omega}_k$. Whereas, for $d/r_H = 1$

there are some periodic shadow points. Moreover, the maximum amount of $\mathcal{C}_{\mathcal{I}_{\omega_k}}$ dampens as $\bar{\omega}_k$ increases in successive periods. Although, in this case we are getting shadow points but it is possible to get shadow regions for large values of d/r_H . This will be clarified in a short while. Interestingly, this periodicity is not due to the $\mathcal{I}_{j_{\omega_k}}$ (see Fig. 3). Whereas, it can be observed from Fig. 4 that $|\mathcal{I}_{\mathcal{E}_{\omega_k}}|$ provides the major contribution in the concurrence and also has similar periodicity. Therefore, this periodic nature of $\mathcal{C}_{\mathcal{I}_{\omega_k}}$ for $d \neq 0$ as a function of $\bar{\omega}_k$ is due to the non-local term.

On the other hand, in Fig. 5 we have plotted $\mathcal{C}_{\mathcal{I}_{\omega_k}}/r_H^2$ as a function of the dimensionless transition energy $\Delta\bar{E} = r_H\Delta E$ of the detectors for fixed $\bar{\omega}_k = 1$ and for $d/r_H = 0$ and $d/r_H = 1$ respectively, where $\Delta E = \Delta E^A = \Delta E^B$. These plots also proclaim the possibility of entanglement harvesting for low values of ΔE . We also see that the amount of harvested entanglement decreases with increasing detector transition energy. Fig. 6 and Fig. 7 confirm that major contribution in concurrence comes from $|\mathcal{I}_{\mathcal{E}_{\omega_k}}|$ rather than $\mathcal{I}_{j_{\omega_k}}$.

Next in Fig. 8 we have plotted $\mathcal{C}_{\mathcal{I}_{\omega_k}}/r_H^2$ with respect to the dimensionless distance d/r_H between the two detectors' null trajectories for fixed $\Delta\bar{E} = 0.5$ and different $\bar{\omega}_k$ respectively. These plots and corresponding numerical values confirm that entanglement harvesting is happening in a periodic manner with respect to d/r_H , with period depending on $\bar{\omega}_k$. We observe that this period decreases with increasing values of $\bar{\omega}_k$. They also confirm that there are periodic d/r_H values where harvesting stops, i.e., $\mathcal{C}_{\mathcal{I}_{\omega_k}}/r_H^2$ becomes zero. We further observed that for small $\bar{\omega}_k$ ($= 0.05, 0.1$) there are entanglement harvesting shadow regions while for $\bar{\omega}_k$ ($= 1, 2$) these regions become point-like. This figure also confirms that for large d values $\mathcal{C}_{\mathcal{I}_{\omega_k}}/r_H^2$ as a function of $\bar{\omega}_k$ shows shadow regions rather than points, which we was promised to be shown earlier. The entanglement har-

vesting shadow regions have also been observed earlier in the case of black holes [26, 54]. However, in [26] and [54], the entanglement harvesting shadow regions are observed in different spacetimes, related to the analysis near the event horizons of static and rotating BTZ black holes, respectively.

2. Unruh vacuum

Here we consider the Wightman function estimated with the Unruh vacuum from Eq. (33) to estimate integrals of (7) to investigate the entanglement harvesting condition. In particular, one can find out the individual detector transition probabilities \mathcal{I}_j as

$$\begin{aligned}\mathcal{I}_j &= \int_{-\infty}^{\infty} dt'_j \int_{-\infty}^{\infty} dt_j e^{-i\Delta E^j(t'_j - t_j)} G_B^+(X'_j, X_j) \\ &= \int_0^{\infty} \frac{d\omega_k}{4\pi\omega_k} \mathcal{I}_{j_{\omega_k}},\end{aligned}\quad (55)$$

where $\mathcal{I}_{j_{\omega_k}}$ are now given by

$$\begin{aligned}\mathcal{I}_{j_{\omega_k}} &= \int_{-\infty}^{\infty} dt'_j \int_{-\infty}^{\infty} dt_j e^{-i\Delta E^j(t'_j - t_j)} \\ &\quad \times [e^{-i\omega_k(U_{j'} - U_j)} + e^{-i\omega_k(v_{j'} - v_j)}].\end{aligned}\quad (56)$$

With the help of Eq. (34) and (35) one can observe that this integral is same as the one from Eq. (43) of the Boulware vacuum case. Then this should also provide the same result of Eq. (46). Let us now evaluate the integrals $\mathcal{I}_{\mathcal{E}_{\omega_k}}^W$ and $\mathcal{I}_{\mathcal{E}_{\omega_k}}^R$ from (48) and (49) with the Green's functions (33) evaluated from the Unruh vacuum. First let us proceed to calculate $\mathcal{I}_{\mathcal{E}_{\omega_k}}^W$, which in this case turns out to be

$$\begin{aligned}\mathcal{I}_{\mathcal{E}_{\omega_k}}^W &= \int_{-\infty}^{\infty} dt_B \int_{-\infty}^{\infty} dt_A e^{i(\Delta E^B t_B + \Delta E^A t_A)} [e^{-i\omega_k(U_B - U_A)} + e^{-i\omega_k(v_B - v_A)}] \\ &= \int_{-\infty}^{\infty} dt_B \int_{-\infty}^{\infty} dt_A e^{i(\Delta E^B t_B + \Delta E^A t_A)} \left[\exp \left\{ i\omega_k 2r_H \left(1 - e^{-\frac{d}{2r_H}} \right) \right\} + e^{-i\omega_k(2r_B - 2r_A - d)} \left(\frac{r_B - r_H}{r_A - r_H} \right)^{-2ir_H\omega_k} \right]\end{aligned}\quad (57)$$

The integration with the first term inside the square bracket will vanish due to the Dirac delta distributions $\delta(\Delta E^j)$, with $\Delta E^j > 0$. Then this integral becomes ex-

actly same with the one for the Boulware vacuum from Eq. (51). On the other hand, in a similar manner one can evaluate the quantity $\mathcal{I}_{\mathcal{E}_{\omega_k}}^R$ as

$$\begin{aligned}\mathcal{I}_{\mathcal{E}_{\omega_k}}^R &= \int_{-\infty}^{\infty} dt_A \int_{-\infty}^{\infty} dt_B e^{i(\Delta E^B t_B + \Delta E^A t_A)} \left[\theta(t_{s_A} - t_{s_B}) \{ e^{-i\omega_k(v_A - v_B)} - e^{-i\omega_k(v_B - v_A)} \} \right. \\ &\quad \left. + \theta(T_{K_A} - T_{K_B}) \{ e^{-i\omega_k(U_A - U_B)} - e^{-i\omega_k(U_B - U_A)} \} \right]\end{aligned}$$

$$\begin{aligned}
&= \int_{r_H}^{\infty} dr_A \frac{r_A + r_H}{r_A - r_H} \int_{r_H}^{r_A} dr_B \frac{r_B + r_H}{r_B - r_H} e^{i\{\Delta E^B r_B + \Delta E^A (r_A + d)\}} \left(\frac{r_B}{r_H} - 1\right)^{2ir_H \Delta E^B} \left(\frac{r_A}{r_H} - 1\right)^{2ir_H \Delta E^A} \\
&\quad \times \left[e^{-i\omega_k(2r_A + d - 2r_B)} \left(\frac{r_A - r_H}{r_B - r_H}\right)^{-2ir_H \omega_k} - e^{-i\omega_k(2r_B - 2r_A - d)} \left(\frac{r_B - r_H}{r_A - r_H}\right)^{-2ir_H \omega_k} - 2i \sin \left\{ \omega_k 2r_H \left(1 - e^{-\frac{d}{2r_H}}\right) \right\} \right].
\end{aligned} \tag{58}$$

Here we note that while dealing with modes which are represented in terms of the EF null coordinates the Heaviside step function arising from the Feynman propagator should take the time to be the Schwarzschild time t_s . While for modes which are represented in terms of the Kruskal null coordinates (U, V) , one should take the relevant time to be the Kruskal time $T_K = (U + V)/2$. This Kruskal time is expressed in terms of the Schwarzschild time and the tortoise coordinate as $T_K = 2r_H e^{r_*/2r_H} \sinh(t_s/2r_H)$. Using this expression and the null paths followed by Alice and Bob as $t_{sA} - r_{sA} = d > 0$ and $t_{sB} - r_{sB} = 0$, respectively one finds that $T_{KA} > T_{KB}$ implies $r_A > r_B$ (see Appendix B). Therefore the Heaviside function $\theta(T_{KA} - T_{KB})$ can be replaced by $\theta(r_A - r_B)$. Similarly, as explained earlier, $t_{sA} > t_{sB}$ implies $r_A > r_B$ and hence we replace $\theta(t_{sA} - t_{sB})$ by $\theta(r_A - r_B)$. Using these the last result of (58) has been obtained. We observe that the expression of $\mathcal{I}_{\varepsilon_{\omega_k}}^R$ from Eq. (58) and (54) are mathematically same except for the last term. In Appendix A 2 we have shown that this last term $2i \sin \left\{ \omega_k 2r_H \left(1 - e^{-d/2r_H}\right) \right\}$ is many order smaller than the rest of the expressions for the same set of parameter values. Therefore, the nature of entanglement harvesting with respect to the Unruh vacuum is similar to that in the Boulware vacuum.

B. de Sitter universe

1. (1 + 1)–dimensions

Let us now evaluate the integrals of Eq. (4) for detectors in null trajectories in a de Sitter spacetime, so that one can check the entanglement condition (7) and also quantify the harvested entanglement using (10). In this regard, we first consider the integral \mathcal{I}_j , which using the Green's function of Eq. (37) is represented as

$$\begin{aligned}
\mathcal{I}_j &= \int_{-\infty}^{\infty} dt'_j \int_{-\infty}^{\infty} dt_j e^{-i\Delta E^j(t'_j - t_j)} G_D^+(X'_j, X_j) \\
&= \int_0^{\infty} \frac{d\omega_k}{4\pi\omega_k} \mathcal{I}_{j\omega_k}.
\end{aligned} \tag{59}$$

Here the detector times τ_j are represented by the de Sitter coordinate times t_j . Like the previous Schwarzschild case here also we shall be evaluating $\mathcal{I}_{j\omega_k}$, which correspond to a certain frequency of the field mode, to arrive at the entanglement harvesting condition. With the con-

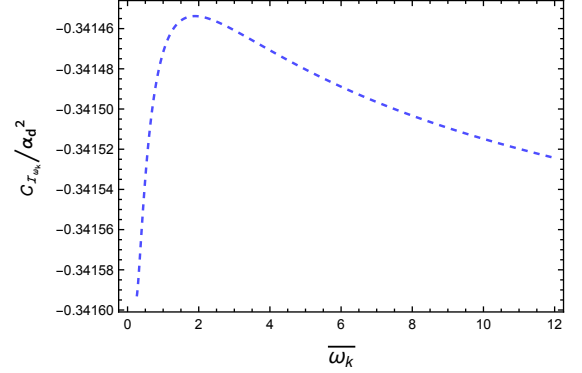


FIG. 9: The quantity $\mathcal{C}_{\mathcal{I}_{\omega_k}}/\alpha_d^2$, signifying the concurrence, is plotted for two outgoing null detectors in a (1 + 1) dimensional de Sitter spacetime with respect to the dimensionless frequency of the field $\bar{\omega}_k = \omega_k \alpha_d$ for fixed dimensionless detector transition energy $\bar{\Delta E} = \Delta E \alpha_d = 0.5$. The other fixed parameter is $d/\alpha_d = 0$.

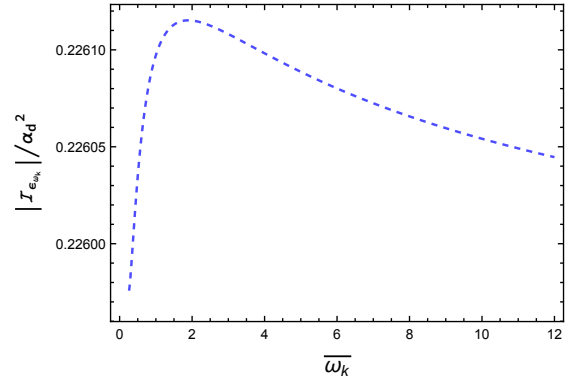


FIG. 10: The quantity $|\mathcal{I}_{\varepsilon_{\omega_k}}|/\alpha_d^2$ is plotted for two outgoing null detectors in a (1 + 1) dimensional de Sitter spacetime with respect to the dimensionless frequency of the field $\bar{\omega}_k$ for fixed $\bar{\Delta E} = 0.5$ and $d/\alpha_d = 0$.

sideration of outgoing null paths for both Alice and Bob one can express the integrals $\mathcal{I}_{j\omega_k}$ as

$$\begin{aligned}
\mathcal{I}_{j\omega_k} &= \int_{-\infty}^{\infty} dt'_j \int_{-\infty}^{\infty} dt_j e^{-i\Delta E^j(t'_j - t_j)} \\
&\quad \times \left[e^{2i\omega_k \alpha_d (e^{-t'_j/\alpha_d} - e^{-t_j/\alpha_d})} + 1 \right].
\end{aligned} \tag{60}$$

Here one can observe that the integration over the second additive unity is simple and provides multiplicative factors of the Dirac delta distribution $\delta(\Delta E^j)$. For non zero

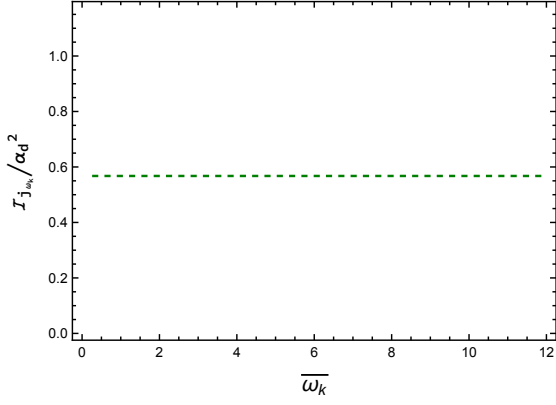


FIG. 11: The quantity $\mathcal{I}_{j_{\omega_k}}/\alpha_d^2$, signifying the individual detector transition probability, is plotted as a function of the dimensionless frequency of the field $\bar{\omega}_k$ for a detector in an outgoing null path in a $(1+1)$ dimensional de Sitter spacetime. The dimensionless transition energy of the detector is fixed at $\Delta\bar{E} = 0.5$. From this figure, one can notice that the individual detector transition probability, in this case, is independent of the frequency of the field $\bar{\omega}_k$. From (63) one should note that they are also independent of d/α_d .

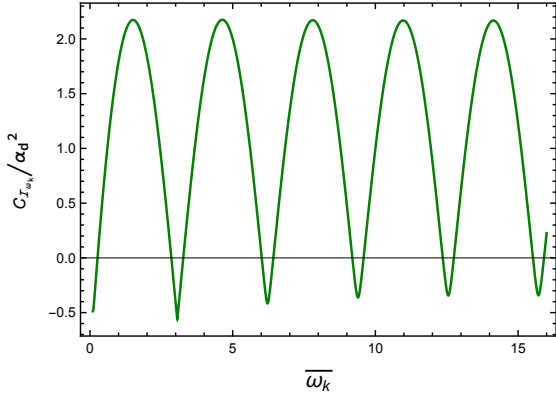


FIG. 12: The quantity $\mathcal{C}_{\mathcal{I}_{\omega_k}}/\alpha_d^2$, signifying the concurrence, is plotted for two outgoing null detectors in a $(1+1)$ dimensional de Sitter spacetime with respect to the dimensionless frequency of the field $\bar{\omega}_k$ for fixed dimensionless detector transition energy $\Delta\bar{E} = 0.5$, and fixed $d/\alpha_d = 1$.

detector transition energy $\Delta E^j > 0$ these quantities are bound to make the concerned part of the integral vanish. Then the previous integral with the change of variables $e^{-t/\alpha_d} = z$ can be evaluated as

$$\mathcal{I}_{j_{\omega_k}} = \alpha_d^2 \left| \int_0^\infty dz z^{i\Delta E^j \alpha_d - 1} e^{2i\omega_k \alpha_d z} \right|^2. \quad (61)$$

To evaluate this integral we introduce regulators of the form $(z^\epsilon e^{-\epsilon z})$, where ϵ is a positive real parameter with $\epsilon \ll 1$. One can get the actual value of the integral by taking the limit $\epsilon \rightarrow 0$ after evaluating the regulated integral as

$$\lim_{\epsilon \rightarrow 0} \left[\int_0^\infty dz z^{i\Delta E^j \alpha_d - 1 + \epsilon} e^{(2i\omega_k \alpha_d - \epsilon)z} \right]$$

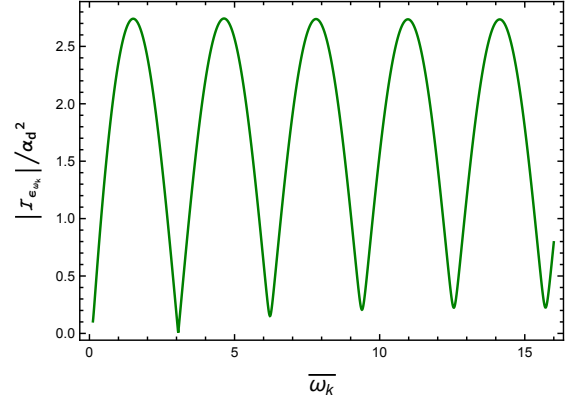


FIG. 13: The quantity $|\mathcal{I}_{\epsilon_{\omega_k}}|/\alpha_d^2$ is plotted for two outgoing null detectors in a $(1+1)$ dimensional de Sitter spacetime with respect to the dimensionless frequency of the field $\bar{\omega}_k$ for fixed $\Delta\bar{E} = 0.5$, and $d/\alpha_d = 1$.

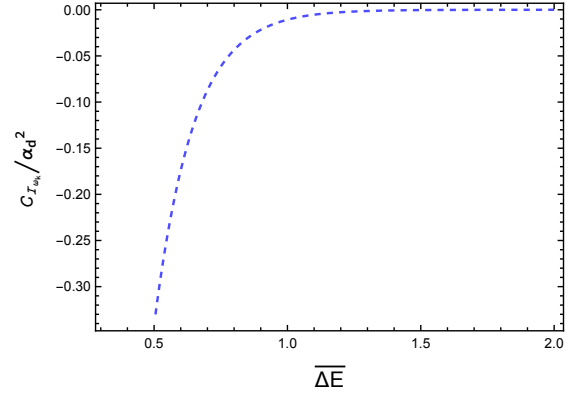


FIG. 14: The quantity $\mathcal{C}_{\mathcal{I}_{\omega_k}}/\alpha_d^2$, signifying the concurrence, is plotted for two outgoing null detectors in a $(1+1)$ dimensional de Sitter spacetime with respect to the dimensionless transition energy $\Delta\bar{E}$ of the detectors for fixed dimensionless frequency of the field $\bar{\omega}_k = 0.2$, and fixed $d/\alpha_d = 0$.

$$= e^{-\pi\alpha_d\Delta E^j/2} (2\omega_k\alpha_d)^{-i\alpha_d\Delta E^j} \Gamma(i\alpha_d\Delta E^j). \quad (62)$$

Then one can promptly express $\mathcal{I}_{j_{\omega_k}}$ as

$$\mathcal{I}_{j_{\omega_k}} = \frac{2\pi\alpha_d}{\Delta E^j} \frac{1}{e^{2\pi\alpha_d\Delta E^j} - 1}, \quad (63)$$

where we have used the *Gamma function* identity $\Gamma(iz)\Gamma(-iz) = \pi/(z \sinh \pi z)$. Let us now evaluate the integral \mathcal{I}_ϵ , which can again be expressed as

$$\mathcal{I}_\epsilon = - \int_0^\infty \frac{d\omega_k}{4\pi\omega_k} \left[\mathcal{I}_{\epsilon_{\omega_k}}^W + \mathcal{I}_{\epsilon_{\omega_k}}^R \right], \quad (64)$$

which is in same way that we have considered in the Schwarzschild case. Here, one can evaluate the quantity $\mathcal{I}_{\epsilon_{\omega_k}}^W$ as

$$\mathcal{I}_{\epsilon_{\omega_k}}^W = \int_{-\infty}^\infty dt_B \int_{-\infty}^\infty dt_A e^{i(\Delta E^A t_A + \Delta E^B t_B)}$$

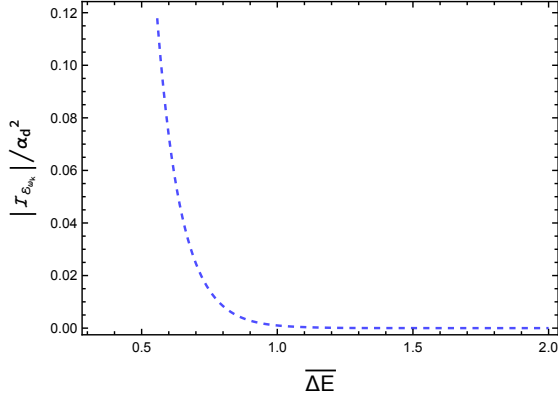


FIG. 15: The quantity $|I_{\epsilon_{\omega_k}}|/\alpha_d^2$ is plotted for two outgoing null detectors in a $(1+1)$ dimensional de Sitter spacetime with respect to the dimensionless transition energy ΔE of the detectors for fixed dimensionless frequency of the field $\bar{\omega}_k = 0.2$, and fixed $d/\alpha_d = 0$.

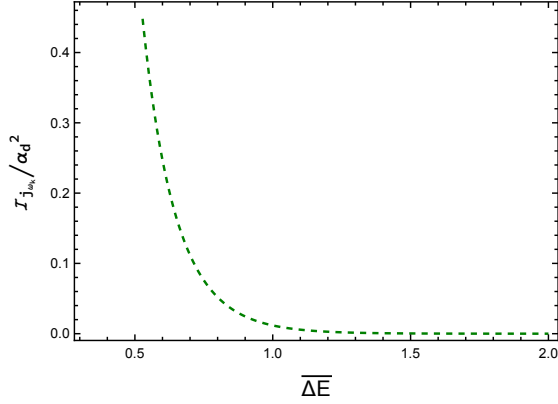


FIG. 16: The quantity $I_{j_{\omega_k}}/\alpha_d^2$ is plotted for two outgoing null detectors in a $(1+1)$ dimensional de Sitter spacetime with respect to the dimensionless transition energy ΔE of the detectors for fixed dimensionless frequency of the field $\bar{\omega}_k = 0.2$. This nature will be the same for all d/α_d values as the quantity is independent of d .

$$\begin{aligned} & \times \left\{ e^{-i\omega_k(u_B - u_A)} + e^{-i\omega_k(v_B - v_A)} \right\} \\ &= \int_{-\infty}^{\infty} dt_B \int_{-\infty}^{\infty} dt_A e^{i(\Delta E^A t_A + \Delta E^B t_B)} \\ & \times \left[e^{i\omega_k d} + e^{-i\omega_k d} e^{2i\omega_k \alpha_d (e^{-t_B/\alpha_d} - e^{-t_A/\alpha_d})} \right]. \end{aligned} \quad (65)$$

Here also one can observe that the integration over the first quantity with $e^{i\omega_k d}$ as multiplicative factor will provide the multiplication of Dirac delta distributions $\delta(\Delta E^A)$ and $\delta(\Delta E^B)$. Therefore that part of the integral will vanish as the detector transition energy $\Delta E^j > 0$. Now with the change of variables $z_j = e^{-t_j/\alpha_d}$ one simplifies the previous integral as

$$\begin{aligned} \mathcal{I}_{\epsilon_{\omega_k}}^W &= \alpha_d^2 e^{-i\omega_k d} \int_0^\infty dz_A \int_0^\infty dz_B e^{2i\omega_k \alpha_d (z_B - z_A)} \\ & \times z_A^{-i\Delta E^A \alpha_d - 1} z_B^{-i\Delta E^B \alpha_d - 1}. \end{aligned} \quad (66)$$

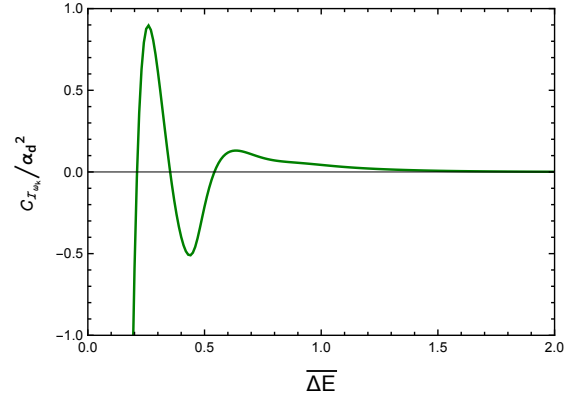


FIG. 17: The quantity $C_{I_{\omega_k}}/\alpha_d^2$, signifying the concurrence, is plotted for two outgoing null detectors in a $(1+1)$ dimensional de Sitter spacetime with respect to the dimensionless transition energy ΔE of the detectors for fixed dimensionless frequency of the field $\bar{\omega}_k = 0.2$, and fixed $d/\alpha_d = 1$.

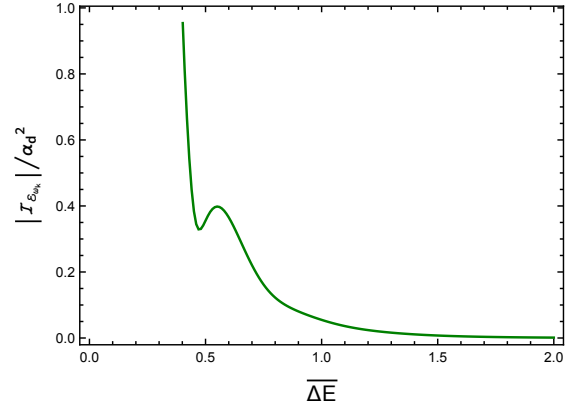


FIG. 18: The quantity $|I_{\epsilon_{\omega_k}}|/\alpha_d^2$ is plotted for two outgoing null detectors in a $(1+1)$ dimensional de Sitter spacetime with respect to the dimensionless transition energy ΔE of the detectors for fixed dimensionless frequency of the field $\bar{\omega}_k = 0.2$, and fixed $d/\alpha_d = 1$.

By introducing regulators of the form $(z_A z_B)^\epsilon e^{-\epsilon(z_A + z_B)}$, with a positive real parameter ϵ , one can evaluate this integral. The explicit expression after the integration is carried out, is provided in the Appendix. C1. We now proceed to evaluate the integral $\mathcal{I}_{\epsilon_{\omega_k}}^R$, which can be expressed as

$$\begin{aligned} \mathcal{I}_{\epsilon_{\omega_k}}^R &= \int_{-\infty}^{\infty} dt_B \int_{-\infty}^{\infty} dt_A e^{i(\Delta E^A t_A + \Delta E^B t_B)} \theta(\eta_A - \eta_B) \\ & \times \left\{ e^{-i\omega_k(u_A - u_B)} + e^{-i\omega_k(v_A - v_B)} \right. \\ & \quad \left. - e^{-i\omega_k(u_B - u_A)} - e^{-i\omega_k(v_B - v_A)} \right\} \\ &= \alpha_d^2 \int_0^\infty dz_A \int_{z_A}^\infty dz_B z_A^{-i\Delta E^A \alpha_d - 1} z_B^{-i\Delta E^B \alpha_d - 1} \\ & \times \left\{ e^{i\omega_k d} e^{2i\omega_k \alpha_d (z_A - z_B)} - e^{-i\omega_k d} e^{2i\omega_k \alpha_d (z_B - z_A)} \right\} \end{aligned}$$

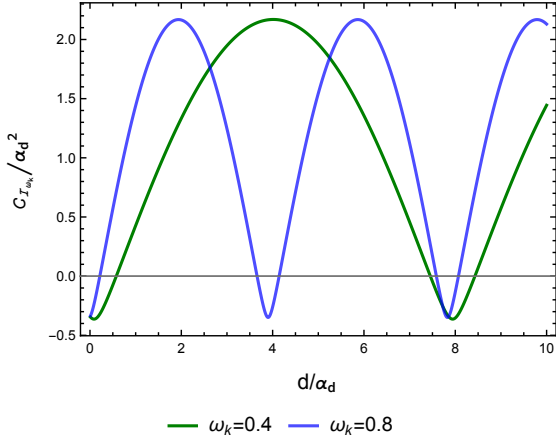


FIG. 19: The quantity $\mathcal{C}_{\mathcal{I}_{\omega_k}}/\alpha_d^2$ is plotted for two outgoing null detectors in different parallel paths in a $(1+1)$ dimensional de-Sitter spacetime with respect to the separation between the two paths d/α_d for different dimensionless frequencies of the field. The detector transition energies are fixed at $\Delta E = 0.5$.

$$-2i \sin \omega_k d \}. \quad (67)$$

In de Sitter background, the real scalar field is decomposed with respect to the positive and negative frequency modes, represented in the conformal time η . Therefore, the time T_j inside the Heaviside step function here is denoted by the conformal time. Here for positive α_d one obtains $\theta(\eta_A - \eta_B) = \theta(t_A - t_B) = \theta(z_B - z_A)$ using the relation (21), and we have used this fact to realize the previous expression. We also mention that utilization of the function $\theta(z_B - z_A)$ transformed the z_B integration range from $[0, \infty)$ to $[z_A, \infty)$ in the representation of Eq. (67). This integral can be evaluated numerically with the introduction of the regulator of the form $(z_A z_B)^\epsilon e^{-\epsilon(z_A + z_B)}$, with positive real ϵ .

In Fig. 9 we have plotted the dimensionless quantity $\mathcal{C}_{\mathcal{I}_{\omega_k}}/\alpha_d^2$, representing the concurrence, as a function of the dimensionless frequency $\bar{\omega}_k = \omega_k \alpha_d$ for fixed $\Delta E^A = \alpha_d \Delta E^A = 0.5$, $\Delta E^B = \alpha_d \Delta E^B = 0.5$, and $d = 0$. This plot asserts that entanglement harvesting is not possible when the detectors move along the same path. We observe from Fig. 10 and 11 that here $\mathcal{I}_{j\omega_k}$ is larger than $|\mathcal{I}_{\varepsilon\omega_k}|$ and as a result $(|\mathcal{I}_{\varepsilon}| - \sqrt{\mathcal{I}_A \mathcal{I}_B})/\alpha_d^2$ is negative. However, Fig. 12, obtained for the same parameters but $d/\alpha_d = 1$, shows that $\mathcal{C}_{\mathcal{I}_{\omega_k}}/r_H^2$ is now positive making entanglement harvesting possible in this scenario. Moreover, one observes that there are periodic entanglement harvesting regions with respect to frequency $\bar{\omega}_k$. Like earlier case here also this periodicity is only due to $|\mathcal{I}_{\varepsilon\omega_k}|$, see Fig. 11 and 13.

We now plot $\mathcal{C}_{\mathcal{I}_{\omega_k}}/\alpha_d^2$ with respect to the dimensionless transition energy ΔE of the detectors for fixed $\bar{\omega}_k = 0.2$ and $d = 0$ in Fig. 14. This plot also states that for $d = 0$ the entanglement harvesting is not possible. This claim is supported by Fig. 15 and 16. However, from

Fig. 17 with 18, where the similar plots are obtained for $d/\alpha_d = 1$, we observe that entanglement harvesting is possible in certain discrete ranges of ΔE .

Finally in Fig. 19 we plot the concurrence $\mathcal{C}_{\mathcal{I}_{\omega_k}}/\alpha_d^2$ with respect to d/α_d for fixed $\Delta E = 0.5$ and different $\bar{\omega}_k$. This plot is consistent with the findings of Fig. 9 and Fig. 14, reconfirming that for $d/\alpha_d = 0$ harvesting is not possible. Fig. 19 indicates that like the Schwarzschild case here also harvesting is periodic with respect to d/α_d . Here also one perceives the occurrence of entanglement harvesting shadow regions, the length of which decreases with increasing frequency $\bar{\omega}_k$. However, here we have seen that with increasing $\bar{\omega}_k$ (in the range $[10^{-4}, 10^4]$) the shadow regions do not become shadow points.

2. $(1+3)$ -dimensions

In $(1+3)$ -dimensional de Sitter spacetime one can express the integrals from Eq. (4), essential for perceiving the entanglement harvesting (7), as

$$\begin{aligned} \mathcal{I}_j &= \int_{-\infty}^{\infty} dt'_j \int_{-\infty}^{\infty} dt_j e^{-i\Delta E^j(t'_j - t_j)} G_D^+(X'_j, X_j) \\ &= \int \frac{d^2 k_{\perp}}{(2\pi)^3 2\omega_k} \int_0^{\infty} dk_x \mathcal{I}_{j\omega_k}, \end{aligned} \quad (68)$$

where, $\omega_k^2 = k_{\perp}^2 + k_x^2$, and $k_{\perp}^2 = k_y^2 + k_z^2$. These integrations over t'_j , and t_j can be solved for detectors in outgoing null paths using the Green's functions (40) as

$$\begin{aligned} \mathcal{I}_{j\omega_k} &= \int_{-\infty}^{\infty} dt'_j \int_{-\infty}^{\infty} dt_j \frac{e^{-i\Delta E^j(t'_j - t_j)}}{a(\eta'_j)a(\eta_j)} \\ &\times \left[e^{ik_x \Delta x_{j'j} - i\omega_k \Delta \eta_{j'j}} + e^{-ik_x \Delta x_{j'j} - i\omega_k \Delta \eta_{j'j}} \right] \\ &= \int_{-\infty}^{\infty} dt'_j \int_{-\infty}^{\infty} dt_j e^{-i\Delta E^j(t'_j - t_j)} \\ &\times \frac{1}{e^{t'_j/\alpha_d + t_j/\alpha_d}} \left[e^{i\alpha_d(\omega_k - k_x)(e^{-t'_j/\alpha_d} - e^{-t_j/\alpha_d})} \right. \\ &\quad \left. + e^{i\alpha_d(\omega_k + k_x)(e^{-t'_j/\alpha_d} - e^{-t_j/\alpha_d})} \right]. \end{aligned} \quad (69)$$

With the change of variables $z_j = e^{-t_j/\alpha_d}$ this expression changes into

$$\begin{aligned} \mathcal{I}_{j\omega_k} &= \alpha_d^2 \left[\left| \int_0^{\infty} dz_j z_j^{-i\alpha_d \Delta E^j} e^{-i\alpha_d(\omega_k - k_x)z_j} \right|^2 \right. \\ &\quad \left. + \left| \int_0^{\infty} dz_j z_j^{-i\alpha_d \Delta E^j} e^{-i\alpha_d(\omega_k + k_x)z_j} \right|^2 \right]. \end{aligned} \quad (70)$$

These integrals can be performed using regulators of the form $(z^\epsilon e^{-\epsilon z})$, and in the limit $\epsilon \rightarrow 0$ results in

$$\mathcal{I}_{j\omega_k} = \left[\frac{1}{(\omega_k - k_x)^2} + \frac{1}{(\omega_k + k_x)^2} \right] \pi \alpha_d \Delta E^j$$

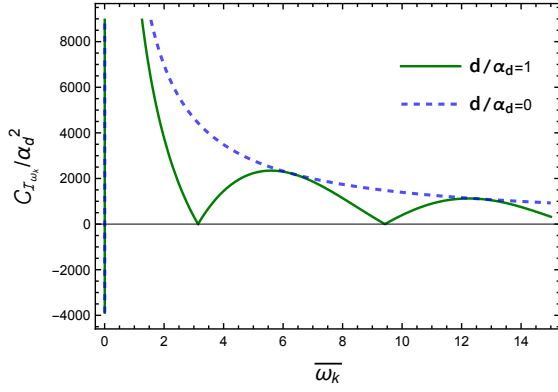


FIG. 20: The quantity $\mathcal{C}_{I_{\omega_k}}/\alpha_d^2$, signifying the concurrence, is plotted for two outgoing null detectors in a (1+3) dimensional de Sitter spacetime with respect to the dimensionless frequency of the field $\bar{\omega}_k = \omega_k \alpha_d$ for fixed dimensionless detector transition energy $\bar{\Delta E} = \Delta E \alpha_d = 0.5$, and fixed $d/\alpha_d = 0$ and $d/\alpha_d = 1$ respectively. We considered $\bar{k}_x = \bar{\omega}_k/2$.

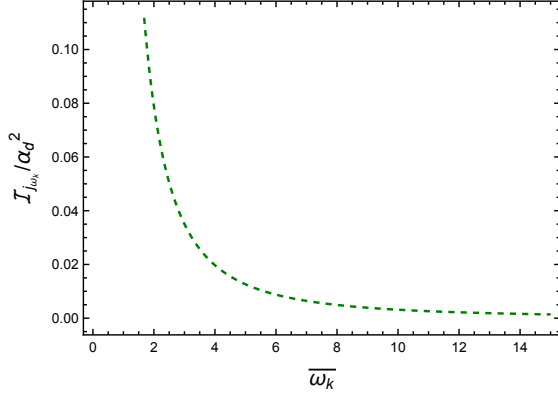


FIG. 21: The quantity $\mathcal{I}_{I_{\omega_k}}/\alpha_d^2$, signifying the concurrence, is plotted for two outgoing null detectors in a (1+3) dimensional de Sitter spacetime with respect to the dimensionless frequency of the field $\bar{\omega}_k = \omega_k \alpha_d$ for fixed $\bar{\Delta E} = 0.5$. We considered $\bar{k}_x = \bar{\omega}_k/2$. This plot is valid for all the d/α_d values.

$$\times \frac{1}{e^{2\pi\alpha_d\Delta E^j} - 1}. \quad (71)$$

Now one can proceed to evaluate the value of \mathcal{I}_ϵ in a similar manner. In particular \mathcal{I}_ϵ can be expressed as

$$\mathcal{I}_\epsilon = - \int \frac{d^2 k_\perp}{(2\pi)^3 2\omega_k} \int_0^\infty dk_x \left[\mathcal{I}_{\epsilon\omega_k}^W + \mathcal{I}_{\epsilon\omega_k}^R \right]. \quad (72)$$

Here the first integral $\mathcal{I}_{\epsilon\omega_k}^W$, which has emerged due to the Wightman function, is

$$\begin{aligned} \mathcal{I}_{\epsilon\omega_k}^W &= \int_{-\infty}^\infty dt_B \int_{-\infty}^\infty dt_A e^{i(\Delta E^A t_A + \Delta E^B t_B)} \frac{1}{a(\eta_A)a(\eta_B)} \\ &\times \left[e^{ik_x \Delta x_{BA} - i\omega_k \Delta \eta_{BA}} + e^{-ik_x \Delta x_{BA} - i\omega_k \Delta \eta_{BA}} \right]. \end{aligned} \quad (73)$$

With a change of variables $z_j = e^{-t_j/\alpha_d}$ this integral

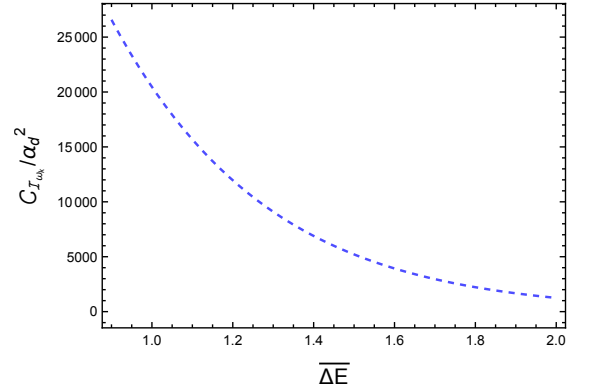


FIG. 22: The quantity $\mathcal{C}_{I_{\omega_k}}/\alpha_d^2$, signifying the concurrence, is plotted for two outgoing null detectors in a (1+3) dimensional de Sitter spacetime with respect to the dimensionless detector transition energy $\bar{\Delta E}$ of the detectors for fixed dimensionless frequency of the field $\bar{\omega}_k = 0.2$, $\bar{k}_x = \bar{\omega}_k/2$, and $d/\alpha_d = 0$.

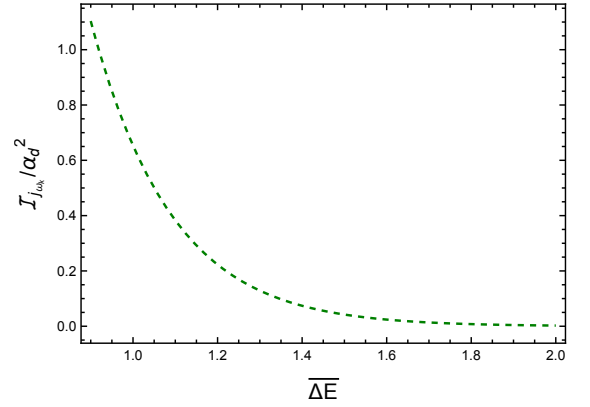


FIG. 23: The quantity $\mathcal{I}_{I_{\omega_k}}/\alpha_d^2$ is plotted for two outgoing null detectors in a (1+3) dimensional de Sitter spacetime with respect to the dimensionless transition energy $\bar{\Delta E}$ of the detectors for fixed $\bar{\omega}_k = 0.2$, and $\bar{k}_x = \bar{\omega}_k/2$. This plot is valid for all the d/α_d values.

turns into

$$\begin{aligned} \mathcal{I}_{\epsilon\omega_k}^W &= \alpha_d^2 \int_0^\infty dz_B \int_0^\infty dz_A z_B^{-i\alpha_d\Delta E^B} z_A^{-i\alpha_d\Delta E^A} \\ &\times \left[e^{i\alpha_d(\omega_k - k_x)(z_B - z_A)} e^{ik_x d} \right. \\ &\quad \left. + e^{i\alpha_d(\omega_k + k_x)(z_B - z_A)} e^{-ik_x d} \right]. \end{aligned} \quad (74)$$

This integral can be straightforwardly evaluated with the introduction of the regulator $(z_A z_B)^\epsilon e^{-\epsilon(z_A + z_B)}$. We mention that the other integral $\mathcal{I}_{\epsilon\omega_k}^R$, arriving from the retarded Green's function, can also be provided a final form in a similar manner after the change of variables as

$$\begin{aligned} \mathcal{I}_{\epsilon\omega_k}^R &= \alpha_d^2 \int_0^\infty dz_A \int_{z_A}^\infty dz_B z_B^{-i\alpha_d\Delta E^B} z_A^{-i\alpha_d\Delta E^A} \\ &\times \left[e^{i\alpha_d(\omega_k - k_x)(z_A - z_B)} e^{-ik_x d} \right. \end{aligned}$$

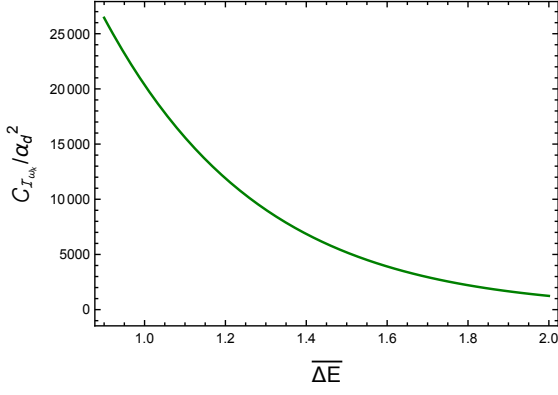


FIG. 24: The quantity $C_{I_{\omega_k}}/\alpha_d^2$, signifying the concurrence, is plotted for two outgoing null detectors in a (1 + 3) dimensional de Sitter spacetime with respect to the dimensionless transition energy $\Delta\bar{E}$ of the detectors for fixed dimensionless frequency of the field $\bar{\omega}_k = 0.2$, $\bar{k}_x = \bar{\omega}_k/2$, and $d/\alpha_d = 1$.

$$\begin{aligned} & + e^{i\alpha_d(\omega_k + k_x)(z_A - z_B)} e^{ik_x d} \\ & - e^{i\alpha_d(\omega_k - k_x)(z_B - z_A)} e^{ik_x d} \\ & - e^{i\alpha_d(\omega_k + k_x)(z_B - z_A)} e^{-ik_x d} \Big], \quad (75) \end{aligned}$$

which can also be evaluated in a similar manner introducing a regulator same as the one in the previous case, see Appendix C 2.

In Fig. 20 we first plot $C_{I_{\omega_k}}/\alpha_d^2$ as a function of $\bar{\omega}_k$ for fixed $\Delta\bar{E}^A = 0.5 = \Delta\bar{E}^B$ and for $d/\alpha_d = 0$ and $d/\alpha_d = 1$ respectively. While in Fig. 21 we have represented the individual detector transition probability with respect to $\bar{\omega}_k$ for the same set of parameters. These plots suggest the possibility of entanglement harvesting in the considered parameter range. For non-zero d/α_d there are periodic entanglement harvesting shadow points with respect to $\bar{\omega}_k$. However, the amplitude of the oscillations keeps decreasing. Like the Schwarzschild case, one can also have shadow regions instead of shadow points for high d values. For $d/\alpha_d = 0$ the plot suggests that entanglement harvesting decreases with increasing field mode frequency. On the other hand, in Fig. 22 we have depicted the concurrence with respect to the dimensionless transition energy $\Delta\bar{E}$ for $d/\alpha_d = 0$ and fixed $\bar{\omega}_k = 0.2$. While the individual detector transition probability is depicted in Fig. 23. Moreover, for $d/\alpha_d = 1$ and for the same other parameters we have depicted the concurrence in Fig. 24. These figures also predict the possibility of entanglement harvesting for the considered parameter ranges, and state that entanglement harvesting decreases with increasing detector transition energy. It should be noted that unlike the (1 + 1) dimensional case in (1 + 3) dimensions entanglement harvesting is possible for $d/\alpha_d = 0$ in similar parameter ranges.

In Fig. 25 we portray the concurrence with respect to the dimensionless distance d/α_d between the two detectors' null trajectories for fixed $\Delta\bar{E} = 0.5$ and different $\bar{\omega}_k$. Like the previous Schwarzschild and (1 + 1) dimensional

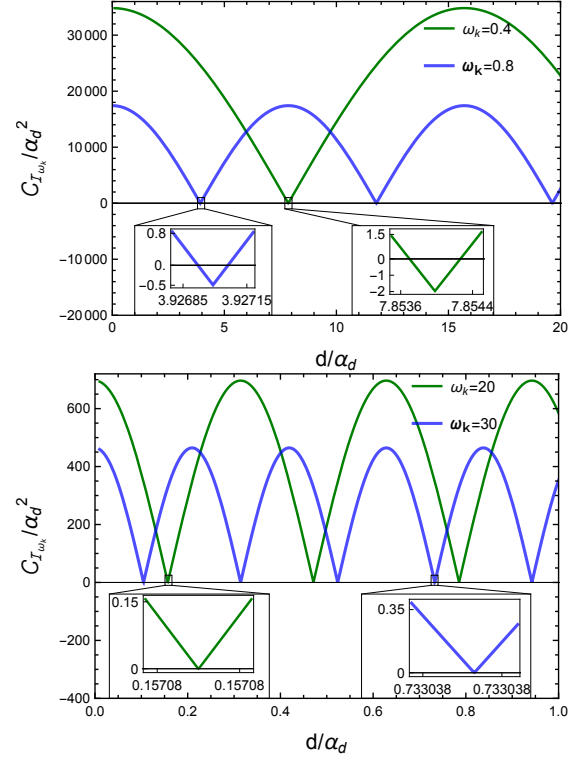


FIG. 25: The quantity $C_{I_{\omega_k}}/\alpha_d^2$ is plotted for two outgoing null detectors in different parallel paths in a (1 + 3) dimensional de-Sitter spacetime with respect to the separation between the two paths d/α_d . The frequency of the field are fixed at $\bar{\omega}_k = 0.4$ and $\bar{\omega}_k = 0.8$, respectively in the upper plot (showing very small shadow regions) and $\bar{\omega}_k = 20$ and $\bar{\omega}_k = 30$, respectively in the lower plot (showing shadow points). Here we fixed $\bar{k}_x = \bar{\omega}_k/2$, and $\Delta\bar{E} = 0.5$.

de Sitter cases these plots show a periodicity of obtained concurrence with respect to d/α_d . However, the plots are more like the Schwarzschild case than the (1 + 1) dimensional de Sitter case. In the present case one periodically perceives entanglement harvesting shadow regions and points in low ($\bar{\omega}_k = 0.4, 0.8$) and high ($\bar{\omega}_k = 20, 30$) frequency regimes respectively. We provide a discussion on the possible reason for these aforesaid similarities between (1 + 1) Schwarzschild and (1 + 3) de Sitter in the discussion section.

VII. QUANTIFICATION OF “TRUE HARVESTING”

So far, we have studied the entanglement harvesting between the two detectors moving in null trajectories in different backgrounds through concurrence. Although the fields are considered in the vacuum state, there is a possibility that the harvested entanglement can have different origins. The reason is the following. We have seen that the concurrence depends on both the local \mathcal{I}_j and non-local \mathcal{I}_ε terms, and both of them depend on the

respective Wightman functions. These Wightman functions can be expressed as a sum of contributions from the commutator and anti-commutator of the field operators. Now since the commutator is proportional to the identity operator, its expectation value is independent of the chosen field state. Hence this part in the non-local term does not confirm whether such contribution to the concurrence is due to the vacuum fluctuations of the field. On the other hand, the expectation value of the anti-commutator is state-dependent. Therefore, this part of the non-local term carries the information about the contribution to the entanglement due to the vacuum fluctuation of the field. Under these circumstances, the former part can be interpreted as harvesting via the communication between the detectors. While the latter part accounts for the entanglement through the vacuum fluctuation of the field even if the detectors are causally disconnected. Therefore, the anti-commutator depending part measures the “true harvesting” [47, 49, 75, 76]. In this scenario, in order to quantify the true harvesting, one should investigate the individual contributions of the commutator and anti-commutator in the \mathcal{I}_ε term of concurrence rather than the same in the \mathcal{I}_j terms, as the former one contains the information about the communication between the two detectors. This idea was first initiated in [75] and later has been used for the black hole case in [47, 49]. A quantitative estimator of true harvesting has been proposed recently in [76].

Inspired by these investigations here we will draw a comparison between the commutator and anti-commutator contributions of the non-local term to understand the role of vacuum fluctuations in the entanglement harvesting. To continue our discussion in this direction we point out that the expression of the integral \mathcal{I}_ε from Eq. (8) can also be cast into the form

$$\mathcal{I}_\varepsilon = -\mathcal{I}_\varepsilon^+ - \mathcal{I}_\varepsilon^- . \quad (76)$$

The quantities $\mathcal{I}_\varepsilon^+$ and $\mathcal{I}_\varepsilon^-$ correspond to integrals which contain the vacuum expectations of the field anti-commutator and commutator exclusively. The explicit expressions of these quantities are

$$\mathcal{I}_\varepsilon^+ = \int_{-\infty}^{\infty} d\tau_B \int_{-\infty}^{\infty} d\tau_A e^{i(\Delta E^B \tau_B + \Delta E^A \tau_A)} \times \{G_W(X_B, X_A) + G_W(X_A, X_B)\}/2; \quad (77)$$

$$\mathcal{I}_\varepsilon^- = \int_{-\infty}^{\infty} d\tau_B \int_{-\infty}^{\infty} d\tau_A e^{i(\Delta E^B \tau_B + \Delta E^A \tau_A)} \times \left[\{G_W(X_B, X_A) - G_W(X_A, X_B)\}/2 + \theta(T_A - T_B) \{G_W(X_A, X_B) - G_W(X_B, X_A)\} \right]. \quad (78)$$

Let us now examine the contribution of which of the terms between $\mathcal{I}_\varepsilon^+$ and $\mathcal{I}_\varepsilon^-$ dominates in the concurrence for different parameter spaces.

A. (1 + 1) dimensional Schwarzschild spacetime

The integrals from Eq. (77) and (78) can be simplified noting that $G_W(X_A, X_B) = G_W^*(X_B, X_A)$. One may also express the integrals in a form $\mathcal{I}_\varepsilon^\pm = \int_0^\infty (d\omega_k/4\pi\omega_k) \mathcal{I}_{\varepsilon\omega_k}^\pm$, which are similar to the ones provided in Eq. (48) and (49). Then the expressions of $\mathcal{I}_{\varepsilon\omega_k}^\pm$ are

$$\begin{aligned} \mathcal{I}_{\varepsilon\omega_k}^+ &= [\mathcal{I}_{\varepsilon\omega_k}^W(\Delta E) + \mathcal{I}_{\varepsilon\omega_k}^{W*}(-\Delta E)]/2, \\ \mathcal{I}_{\varepsilon\omega_k}^- &= [\mathcal{I}_{\varepsilon\omega_k}^W(\Delta E) - \mathcal{I}_{\varepsilon\omega_k}^{W*}(-\Delta E)]/2 + \mathcal{I}_{\varepsilon\omega_k}^R(\Delta E); \end{aligned} \quad (79)$$

where the the integrals $\mathcal{I}_{\varepsilon\omega_k}^W(\Delta E)$ and $\mathcal{I}_{\varepsilon\omega_k}^R(\Delta E)$ are obtained from Eqs. (50) and (52). Now one should note that the quantity $\mathcal{I}_{\varepsilon\omega_k}^+$ is reminiscent of the field anti-commutator and $\mathcal{I}_{\varepsilon\omega_k}^-$ corresponds to the expectation of the field commutator. Following the first discussion of this section one can then assign true harvesting to the contribution of $\mathcal{I}_{\varepsilon\omega_k}^+$. While $\mathcal{I}_{\varepsilon\omega_k}^-$ contributes to the entanglement harvesting through communication channel.

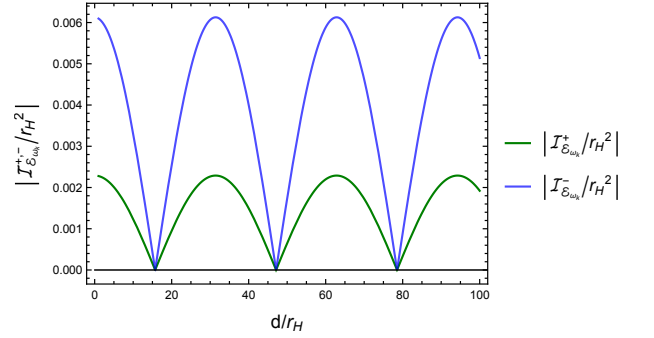


FIG. 26: The quantities $|\mathcal{I}_{\varepsilon\omega_k}^+|/r_H^2$ and $|\mathcal{I}_{\varepsilon\omega_k}^-|/r_H^2$ are plotted in green and blue lines, respectively for two outgoing null detectors in different parallel paths in a (1 + 1) dimensional Schwarzschild black hole spacetime with respect to the separation between the two paths d/r_H . The dimensionless frequency of the field are fixed at $\bar{\omega}_k = 0.1$. The detector transition energy is fixed at $\Delta E = 0.5$.

Let us now discuss the features of these harvesting characterizing quantities. In Fig. 26 and 27 we have plotted the the absolute values of the quantities $\mathcal{I}_{\varepsilon\omega_k}^\pm$ respectively as functions of the the distance d/r_H and the dimensionless frequency $\bar{\omega}_k$. From Fig. 26 one observes that for considered fixed frequency and detector transition energy, the entanglement harvesting is greater through the communication channel. There is a lower contribution from the anti-commutator, which corresponds to true harvesting. However, an interesting thing to note here is that these quantities also vary periodically with the distance d/r_H , and the dips in these quantities are at the same places. From Fig. 27 we see that either of $|\mathcal{I}_{\varepsilon\omega_k}^+|$ or $|\mathcal{I}_{\varepsilon\omega_k}^-|$ may dominate in low

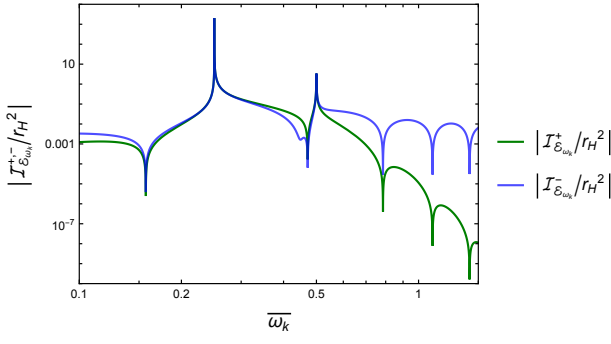


FIG. 27: The quantities $|I_{\varepsilon_{\omega_k}}^+|/r_H^2$ and $|I_{\varepsilon_{\omega_k}}^-|/r_H^2$ are plotted in green and blue lines, respectively for two outgoing null detectors in different parallel paths in a $(1+1)$ dimensional Schwarzschild black hole spacetime with respect to the separation between the two paths d/r_H . The dimensionless frequency of the field are fixed at $d/r_H = 10$. The detector transition energy is fixed at $\Delta E = 0.5$. It should be mentioned that these plots are expressed in *Log-Log* manner for the convenience of representation.

$\bar{\omega}_k$ region and their minima are at the same values of $\bar{\omega}_k$. However, for large $\bar{\omega}_k$ the contribution from $I_{\varepsilon_{\omega_k}}^+$ becomes negligible compared to the other term. Therefore the vacuum fluctuation almost does not play any role for large $\bar{\omega}_k$.

B. $(1+1)$ dimensional de Sitter spacetime

In $(1+1)$ de Sitter spacetime also one can express the integrals $I_{\varepsilon}^{\pm} = \int_0^{\infty} (d\omega_k/4\pi\omega_k) I_{\varepsilon_{\omega_k}}^{\pm}$. The expressions of $I_{\varepsilon_{\omega_k}}^{\pm}$ are given by Eq. (79) and (80). However, here the integrals $I_{\varepsilon_{\omega_k}}^W(\Delta E)$ and $I_{\varepsilon_{\omega_k}}^R(\Delta E)$ are realized from Eq. (65) and (67) for the $(1+1)$ de Sitter case.

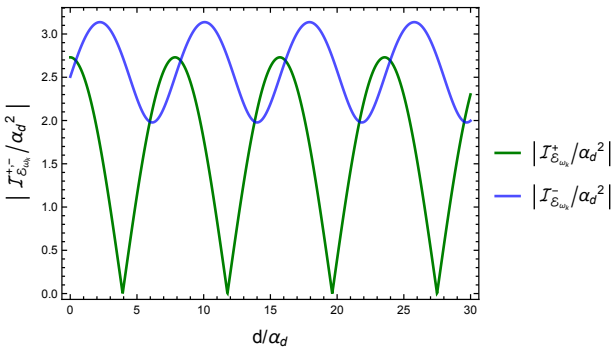


FIG. 28: The quantities $|I_{\varepsilon_{\omega_k}}^+|/r_H^2$ and $|I_{\varepsilon_{\omega_k}}^-|/r_H^2$ are plotted in green and blue lines, respectively for two outgoing null detectors in different parallel paths in a $(1+1)$ dimensional de Sitter spacetime with respect to the separation between the two paths d/r_H . The dimensionless frequency of the field are fixed at $\bar{\omega}_k = 0.4$. The detector transition energy is fixed at $\Delta E = 0.5$.

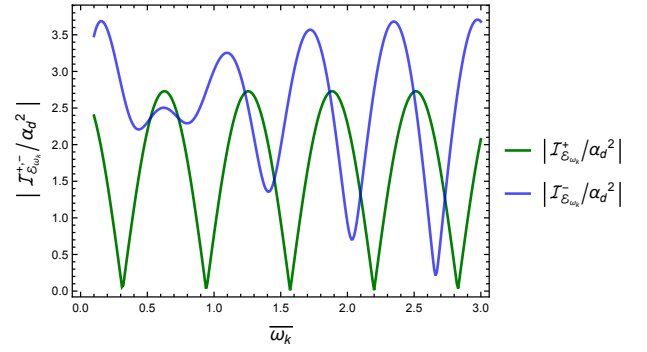


FIG. 29: The quantities $|I_{\varepsilon_{\omega_k}}^+|/r_H^2$ and $|I_{\varepsilon_{\omega_k}}^-|/r_H^2$ are plotted in green and blue lines, respectively for two outgoing null detectors in different parallel paths in a $(1+1)$ dimensional de Sitter spacetime with respect to the separation between the two paths d/r_H . The dimensionless frequency of the field are fixed at $d/\alpha_d = 5$. The detector transition energy is fixed at $\Delta E = 0.5$.

In Fig. 28 and 29 we have plotted the integrals $|I_{\varepsilon_{\omega_k}}^+|$ and $|I_{\varepsilon_{\omega_k}}^-|$ as functions of the dimensionless distance and field frequency respectively. Here the dip in these quantities with respect to d/α_d do not exactly match with the dip in the concurrence, see Fig. 19. This may be due to the fact that unlike the Schwarzschild case, here (see Fig. 28) the $|I_{\varepsilon_{\omega_k}}^+|$ and $|I_{\varepsilon_{\omega_k}}^-|$ do not have the kinks at the same positions. These contributions periodically dominate each other in the total harvesting. From the second Fig. 29 one can observe that the amplitude of the $|I_{\varepsilon_{\omega_k}}^-|$ term is frequency dependent. Here also one observes that the $|I_{\varepsilon_{\omega_k}}^+|$ and $|I_{\varepsilon_{\omega_k}}^-|$ terms dominate each other in different $\bar{\omega}_k$.

C. $(1+3)$ dimensional de Sitter spacetime

In $(1+3)$ de Sitter spacetime we express the integrals $I_{\varepsilon}^{\pm} = \int d^2k_{\perp}/(16\pi^3\omega_k) \int_0^{\infty} dk_x I_{\varepsilon_{\omega_k}}^{\pm}$. The expressions of $I_{\varepsilon_{\omega_k}}^{\pm}$ are again given by Eq. (79) and (80). Here the integrals $I_{\varepsilon_{\omega_k}}^W(\Delta E)$ and $I_{\varepsilon_{\omega_k}}^R(\Delta E)$ are realized from Eqs. (73) and (75) corresponding to the $(1+3)$ dimensional de Sitter case.

In Fig. 30 and 31 we have plotted the integrals $|I_{\varepsilon_{\omega_k}}^{\pm}|$ as functions of the dimensionless distance and field frequency respectively. Like the $(1+1)$ dimensional Schwarzschild case here also we are getting the dips at the same positions for both of these contributions. This is a notable difference from the $(1+1)$ dimensional de Sitter case. However, the current scenario is a bit different from the $(1+1)$ dimensional Schwarzschild case. Here, unlike the Schwarzschild case, $|I_{\varepsilon_{\omega_k}}^+|$ is always many orders lower than $|I_{\varepsilon_{\omega_k}}^-|$. Therefore, most of the entanglement is expected to be harvested through the communication channel.

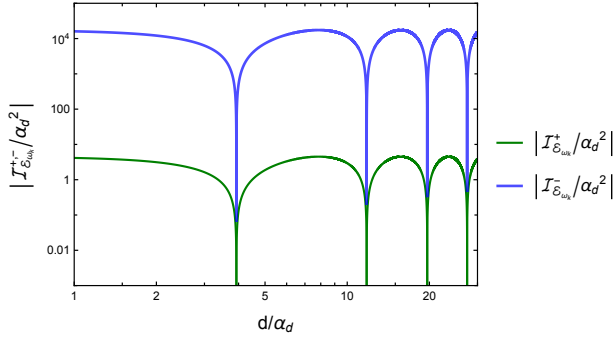


FIG. 30: The quantities $|I_{\mathcal{E}_{\omega_k}}^+ / r_H^2|$ and $|I_{\mathcal{E}_{\omega_k}}^- / r_H^2|$ are plotted in green and blue lines, respectively for two outgoing null detectors in different parallel paths in a (1 + 3) dimensional de Sitter spacetime with respect to the separation between the two paths d/r_H . The dimensionless frequency of the field are fixed at $\bar{\omega}_k = 0.8$. The detector transition energy is fixed at $\Delta E = 0.5$.

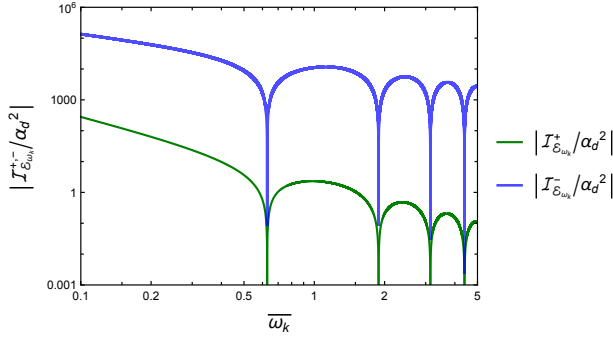


FIG. 31: The quantities $|I_{\mathcal{E}_{\omega_k}}^+ / r_H^2|$ and $|I_{\mathcal{E}_{\omega_k}}^- / r_H^2|$ are plotted in green and blue lines, respectively for two outgoing null detectors in different parallel paths in a (1 + 3) dimensional de Sitter spacetime with respect to the separation between the two paths d/r_H . The dimensionless frequency of the field are fixed at $d/\alpha_d = 5$. The detector transition energy is fixed at $\Delta E = 0.5$.

VIII. MUTUAL INFORMATION

A. In Schwarzschild spacetime with respect to the Boulware and Unruh vacuum

To talk about mutual information of two outgoing null detectors in a Schwarzschild black hole spacetime one needs to evaluate the value of the quantity P_{AB} , thus the integral \mathcal{I}_{AB} . One can express this integral as

$$\begin{aligned} \mathcal{I}_{AB} &= \int_{-\infty}^{\infty} d\tau_B \int_{-\infty}^{\infty} d\tau_A e^{-i(\Delta E^B \tau_B - \Delta E^A \tau_A)} G_W(X_B, X_A) \\ &= \int_0^{\infty} \frac{d\omega_k}{4\pi\omega_k} \mathcal{I}_{AB\omega_k}. \end{aligned} \quad (81)$$

Now we shall be evaluating $\mathcal{I}_{AB\omega_k}$ corresponding to a certain field mode frequency ω_k . In particular considering field mode decomposition corresponding to the Boulware vacuum one can get

$$\begin{aligned} \mathcal{I}_{AB\omega_k} &= \int_{-\infty}^{\infty} d\tau_B \int_{-\infty}^{\infty} d\tau_A e^{-i(\Delta E^B \tau_B - \Delta E^A \tau_A)} \left[e^{i\omega_k d} + e^{-i\omega_k(2r_B - 2r_A - d)} \left(\frac{r_B - r_H}{r_A - r_H} \right)^{-2i\omega_k r_H} \right] \\ &= r_H^2 e^{i(\Delta E^A + \omega_k)d + i(\Delta E^A - \Delta E^B)r_H} \int_0^{\infty} dy_B \frac{y_B + 2}{y_B} \int_0^{\infty} dy_A \frac{y_A + 2}{y_A} \\ &\quad e^{i(\Delta E^A y_A - \Delta E^B y_B)r_H} y_A^{2i\Delta E^A r_H} y_B^{-2i\Delta E^B r_H} \left[1 + e^{-2i\omega_k r_H(y_B - y_A)} \left(\frac{y_B}{y_A} \right)^{-2i\omega_k r_H} \right]. \end{aligned} \quad (82)$$

On the other hand, considering field mode decomposition corresponding to the Unruh vacuum one gets

$$\mathcal{I}_{AB\omega_k} = \int_{-\infty}^{\infty} d\tau_B \int_{-\infty}^{\infty} d\tau_A e^{-i(\Delta E^B \tau_B - \Delta E^A \tau_A)} \left[\exp \left\{ i\omega_k 2r_H \left(1 - e^{-\frac{d}{2r_H}} \right) \right\} + e^{-i\omega_k(2r_B - 2r_A - d)} \left(\frac{r_B - r_H}{r_A - r_H} \right)^{-2i\omega_k r_H} \right]$$

$$\begin{aligned}
&= r_H^2 e^{i\Delta E^A d + i(\Delta E^A - \Delta E^B)r_H} \int_0^\infty dy_B \frac{y_B + 2}{y_B} \int_0^\infty dy_A \frac{y_A + 2}{y_A} e^{i(\Delta E^A y_A - \Delta E^B y_B)r_H} \\
& y_A^{2i\Delta E^A r_H} y_B^{-2i\Delta E^B r_H} \left[\exp \left\{ i\omega_k 2r_H \left(1 - e^{-\frac{d}{2r_H}} \right) \right\} + e^{i\omega_k d} e^{-2i\omega_k r_H (y_B - y_A)} \left(\frac{y_B}{y_A} \right)^{-2i\omega_k r_H} \right]. \quad (83)
\end{aligned}$$

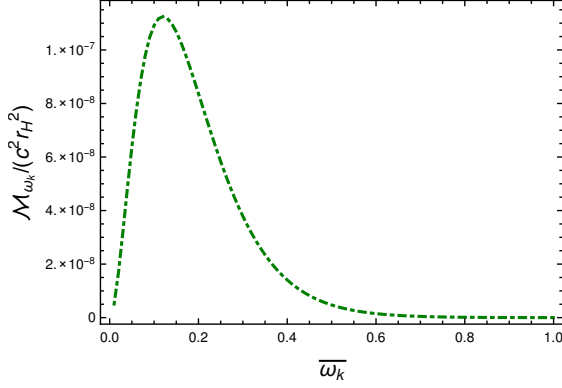


FIG. 32: The mutual information $\mathcal{M}_{\omega_k}(\rho_{AB})/(c^2 r_H^2)$ perceived by two out going null detectors corresponding to the Boulware and Unruh vacuum in plotted with respect to the dimensionless frequency of the field modes $\bar{\omega}_k = r_H \omega_k$ for fixed transition frequency $\Delta \bar{E} = r_H \Delta E = 1$.

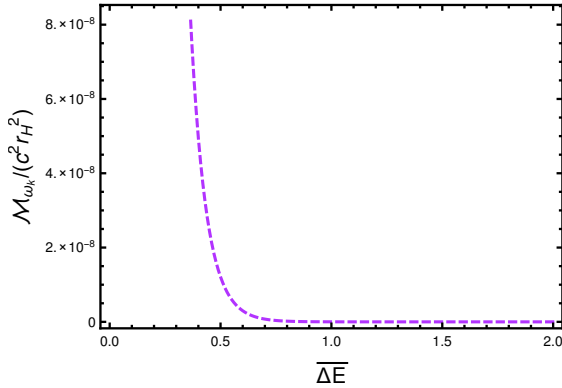


FIG. 33: The mutual information $\mathcal{M}_{\omega_k}(\rho_{AB})/(c^2 r_H^2)$ perceived by two out going null detectors corresponding to the Boulware and Unruh vacuum in plotted with respect to the dimensionless transition frequency $\Delta \bar{E} = r_H \Delta E$ for fixed dimensionless field mode frequency $\bar{\omega}_k = r_H \omega_k = 1$.

One should notice that the first terms in the square brackets on the right hand side of Eq. (82) and (83) vanishes and when $\Delta E^A = \Delta E^B = \Delta E$ both of these integrals get significantly simplified and can be evaluated to be

$$\begin{aligned}
\mathcal{I}_{AB\omega_k} &= e^{i(\Delta E^A + \omega_k)d} \frac{4\pi r_H \omega_k^2}{(\Delta E + \omega_k)(\Delta E + 2\omega_k)^2} \\
&\times \frac{1}{e^{4\pi r_H(\Delta E + \omega_k)} - 1}, \quad (84)
\end{aligned}$$

which is same as $\mathcal{I}_{j\omega_k}$ up-to a phase factor for equal detector transition energies. Now it should be men-

tioned that unlike the expression of the concurrence, the mutual information has multiple disparate multiplicative expectation values of the monopole moment operators $m_j(0)$. In that case one cannot take a common factor of them out from the expression of the mutual information. In particular, from the operator form of $m_j(0) = |E_1^j\rangle\langle E_0^j| + |E_0^j\rangle\langle E_1^j|$ one can get the expectation values $\langle E_1^j | m_j(0) | E_0^j \rangle = 1$. In that case $P_{A\omega_k} = \mathcal{I}_{A\omega_k}$, $P_{B\omega_k} = \mathcal{I}_{B\omega_k}$, and $P_{AB\omega_k} = \mathcal{I}_{AB\omega_k}$, where $P_j = \int_{-\infty}^{\infty} dk / (4\pi\omega_k)$ $P_{j\omega_k}$. For $\Delta E^A = \Delta E^B = \Delta E$, let us consider $\mathcal{I}_{A\omega_k} = \mathcal{I}_{B\omega_k} = |\mathcal{I}_{AB\omega_k}| = \mathcal{I}_{\omega_k}$. Then $P_{+\omega_k} = \mathcal{I}_{\omega_k}$ and $P_{-\omega_k} = 0$, and one can get the mutual information for fixed field frequency ω_k as

$$\mathcal{M}_{\omega_k}(\rho_{AB}) = c^2 2 \mathcal{I}_{\omega_k} \ln 2 + \mathcal{O}(c^4). \quad (85)$$

Therefore we have observed that in both the Boulware and Unruh vacuum cases the mutual information corresponding to a certain field mode frequency up to $\mathcal{O}(c^2)$ are the same and independent of the distance d , between different outgoing null paths. Since mutual information is independent of d and non-vanishing, the correlation is classical at the values of d where entanglement harvesting does not occur. In Fig. 32 and 33 we have plotted the dimensionless mutual information $\mathcal{M}_{\omega_k}(\rho_{AB})/(c^2 r_H^2)$ with respect to the dimensionless parameters $\bar{\omega}_k$ and $\Delta \bar{E}$ respectively. It is observed that the mutual information decreases with increasing detector transition energy.

B. de Sitter universe

1. (1+1)-dimensions

Now we proceed to talk about the mutual information of two outgoing null detectors in a de Sitter background. Again we express the integral $\mathcal{I}_{AB} = \int_0^\infty d\omega_k / (4\pi\omega_k)$ $\mathcal{I}_{AB\omega_k}$ to evaluate P_{AB} . Furthermore, this integral $\mathcal{I}_{AB\omega_k}$ corresponding to the de Sitter vacuum is

$$\begin{aligned}
\mathcal{I}_{AB\omega_k} &= \int_{-\infty}^{\infty} d\tau_B \int_{-\infty}^{\infty} d\tau_A e^{-i(\Delta E^B \tau_B - \Delta E^A \tau_A)} \\
&\left[e^{i\omega_k d} + e^{-i\omega_k d} e^{-2i\omega_k \alpha_d (e^{-\tau_A/\alpha_d} - e^{-\tau_B/\alpha_d})} \right]. \quad (86)
\end{aligned}$$

Like the previous cases here also the integration over $e^{i\omega_k d}$ vanishes using the properties of the Dirac delta distribution for $\Delta E^j > 0$. Then with the change of variables

$e^{-t_j/\alpha_d} = z_j$ the integral $\mathcal{I}_{AB\omega_k}$ becomes

$$\mathcal{I}_{AB\omega_k} = e^{-i\omega_k d} \alpha_d^2 \int_0^\infty dz_B \int_0^\infty dz_A e^{-2i\omega_k \alpha_d (z_A - z_B)} \times z_A^{-i\alpha_d \Delta E^A - 1} z_B^{i\alpha_d \Delta E^B - 1}. \quad (87)$$

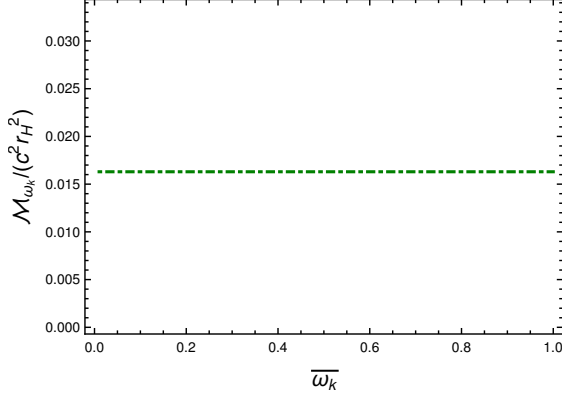


FIG. 34: The mutual information $\mathcal{M}_{\omega_k}(\rho_{AB})/(c^2 \alpha_d^2)$ in (1+1) dimensional de Sitter spacetime as perceived by two out going null detectors is plotted with respect to the dimensionless frequency of the field modes $\bar{\omega}_k = \alpha_d \omega_k$ for fixed transition frequency $\overline{\Delta E} = \alpha_d \Delta E = 1$, and fixed $d/\alpha_d = 0$.

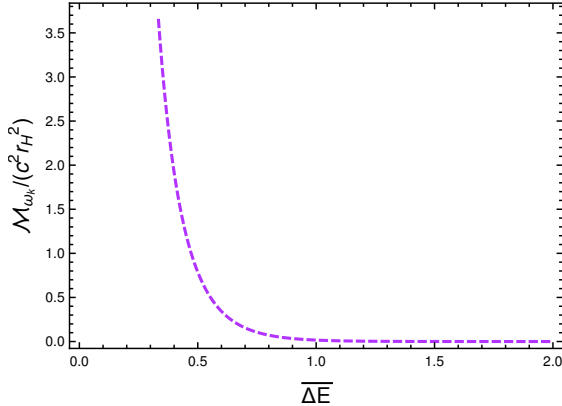


FIG. 35: The mutual information $\mathcal{M}_{\omega_k}(\rho_{AB})/(c^2 r_H^2)$ in (1+1) dimensional de Sitter spacetime as perceived by two out going null detectors is plotted with respect to the dimensionless transition frequency $\overline{\Delta E} = r_H \Delta E$ for fixed dimensionless field mode frequency $\bar{\omega}_k = r_H \omega_k = 1$, and fixed $d/\alpha_d = 0$.

When $\Delta E^A = \Delta E^B = \Delta E$ this integral gets significantly simplified and is evaluated to be

$$\mathcal{I}_{AB\omega_k} = e^{-i\omega_k d} \frac{2\pi\alpha_d}{\Delta E} \frac{1}{e^{2\pi\alpha_d \Delta E} - 1}, \quad (88)$$

which is same as $\mathcal{I}_{j\omega_k}$ up-to a phase factor. In that case one cannot take a common factor of them out from the expression of the mutual information. With the consideration of the form of the monopole moment operator $m_j(0) = |E_1^j\rangle\langle E_0^j| + |E_0^j\rangle\langle E_1^j|$ one gets the

expectation values $\langle E_1^j | m_j(0) | E_0^j \rangle = 1$. In that case $P_{A\omega_k} = \mathcal{I}_{A\omega_k}$, $P_{B\omega_k} = \mathcal{I}_{B\omega_k}$, and $P_{AB\omega_k} = \mathcal{I}_{AB\omega_k}$, where $P_j = \int_{-\infty}^\infty dk / (4\pi\omega_k) P_{j\omega_k}$. For $\Delta E^A = \Delta E^B = \Delta E$, we further consider $\mathcal{I}_{A\omega_k} = \mathcal{I}_{B\omega_k} = |\mathcal{I}_{AB\omega_k}| = \mathcal{I}_{\omega_k}$. Then $P_{+\omega_k} = \mathcal{I}_{\omega_k}$ and $P_{-\omega_k} = 0$, and one can get the mutual information for a certain field frequency ω_k as

$$\mathcal{M}_{\omega_k}(\rho_{AB}) = c^2 2 \mathcal{I}_{\omega_k} \ln 2 + \mathcal{O}(c^4). \quad (89)$$

We observe that this mutual information is independent of the distance d , between different outgoing null paths, and the field mode frequency ω_k , see (63) for \mathcal{I}_{ω_k} . The Mutual information $\mathcal{M}_{\omega_k}(\rho_{AB})/(c^2 r_H^2)$ in this scenario is plotted as functions of $\bar{\omega}_k$ and $\overline{\Delta E}$ respectively in Fig. 34 and 35. From these figures one asserts that mutual information decreases with increasing detector transition energy.

2. (1+3)-dimensions

We are going to evaluate the integral \mathcal{I}_{AB} for the estimation of the quantity P_{AB} . This integral can be further expressed as

$$\begin{aligned} \mathcal{I}_{AB} &= \int_{-\infty}^\infty d\tau_B \int_{-\infty}^\infty d\tau_A e^{-i(\Delta E^B \tau_B - \Delta E^A \tau_A)} G_W(X_B, X_A) \\ &= \int \frac{d^2 k_\perp}{(2\pi)^2 2\omega_k} \int_0^\infty dk_x \mathcal{I}_{AB\omega_k}. \end{aligned} \quad (90)$$

We are now going to evaluate the integral $\mathcal{I}_{AB\omega_k}$ in (1+3) dimensions corresponding to the conformal vacuum as

$$\begin{aligned} \mathcal{I}_{AB\omega_k} &= \int_{-\infty}^\infty d\tau_B \int_{-\infty}^\infty d\tau_A e^{-i(\Delta E^B \tau_B - \Delta E^A \tau_A)} e^{-\frac{t_B + t_A}{\alpha_d}} \\ &\quad \left[e^{ik_x d} e^{i\alpha_d(\omega_k - k_x)} (e^{-t_B/\alpha_d} - e^{-t_A/\alpha_d}) \right. \\ &\quad \left. + e^{-ik_x d} e^{i\alpha_d(\omega_k + k_x)} (e^{-t_B/\alpha_d} - e^{-t_A/\alpha_d}) \right]. \end{aligned} \quad (91)$$

Now one may consider a change of variables $z_j = e^{-t_j/\alpha_d}$. When $\Delta E^A = \Delta E^B = \Delta E$ this integral gets significantly simplified and is evaluated to be

$$\begin{aligned} \mathcal{I}_{AB\omega_k} &= \left[\frac{e^{ik_x d}}{(\omega_k - k_x)^2} + \frac{e^{-ik_x d}}{(\omega_k + k_x)^2} \right] \\ &\quad \times \pi \alpha_d \Delta E \frac{1}{e^{2\pi\alpha_d \Delta E} - 1}. \end{aligned} \quad (92)$$

Unlike the (1 + 1) dimensional case here the integral $\mathcal{I}_{AB\omega_k}$ is not equivalent to $\mathcal{I}_{j\omega_k}$ up-to a phase factor. In (1 + 3) dimensions one also observes that the mutual information will be dependent on the parameter d separating two outgoing null paths. With the expression of the monopole moment operator to be $m_j(0) = |E_1^j\rangle\langle E_0^j| + |E_0^j\rangle\langle E_1^j|$ one gets the expectation values $\langle E_1^j | m_j(0) | E_0^j \rangle = 1$. In that case $P_{A\omega_k} = \mathcal{I}_{A\omega_k}$, $P_{B\omega_k} = \mathcal{I}_{B\omega_k}$, and $P_{AB\omega_k} = \mathcal{I}_{AB\omega_k}$, where

$$P_j = \int \frac{d^2 k_\perp}{(2\pi)^2 2\omega_k} \int_0^\infty dk_x P_{j\omega_k}. \quad (93)$$

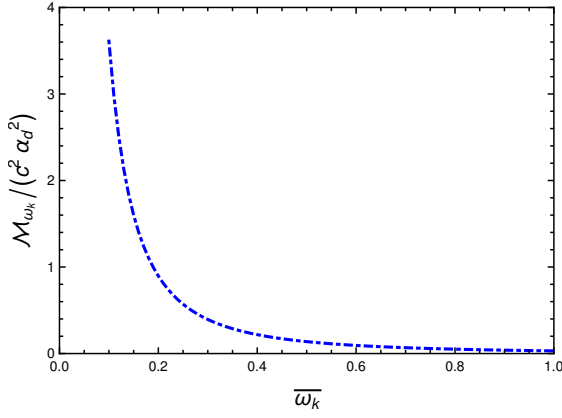


FIG. 36: The mutual information $\mathcal{M}_{\omega_k}(\rho_{AB})/(c^2 r_H^2)$ perceived by two out going null detectors in $(1+3)$ -dimensional de Sitter spacetime corresponding to the conformal vacuum is plotted with respect to the dimensionless frequency of the field modes $\bar{\omega}_k = \alpha_d \omega_k$ for fixed transition frequency $\Delta \bar{E} = \alpha_d \Delta E = 1$, and fixed $d/\alpha_d = 1$. Here we have also considered $\alpha_d k_x = \bar{\omega}_k/2$.

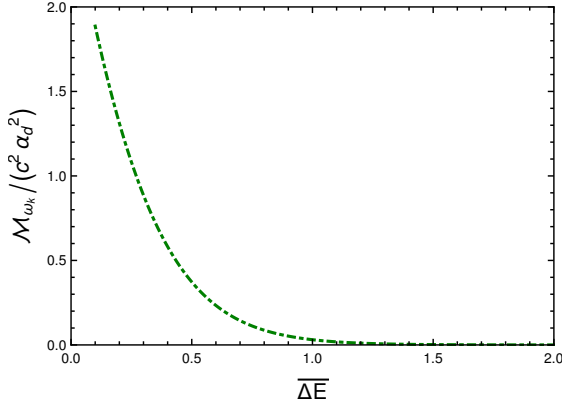


FIG. 37: The mutual information $\mathcal{M}_{\omega_k}(\rho_{AB})/(c^2 r_H^2)$ perceived by two out going null detectors in $(1+3)$ -dimensional de Sitter spacetime corresponding to the conformal vacuum is plotted with respect to the dimensionless transition frequency $\Delta \bar{E} = \alpha_d \Delta E$ for fixed frequency of the field modes and other parameters $\bar{\omega}_k = \alpha_d \omega_k = 1$, $\alpha_d k_x = \bar{\omega}_k/2$ and $d/\alpha_d = 1$.

When $d = 0$ and $\Delta E^A = \Delta E^A = \Delta E$ the integral $\mathcal{I}_{AB\omega_k}$ becomes same with the $\mathcal{I}_{j\omega_k}$. In that scenario one can further consider $\mathcal{I}_{A\omega_k} = \mathcal{I}_{B\omega_k} = |\mathcal{I}_{AB\omega_k}| = \mathcal{I}_{\omega_k}$. Then $P_{+\omega_k} = \mathcal{I}_{\omega_k}$ and $P_{-\omega_k} = 0$, and one can get the mutual information for a certain field frequency ω_k as

$$\mathcal{M}_{\omega_k}(\rho_{AB}) = c^2 2 \mathcal{I}_{\omega_k} \ln 2 + \mathcal{O}(c^4). \quad (94)$$

Then the plots corresponding to $\mathcal{M}_{\omega_k}(\rho_{AB})$ for $d = 0$ should be qualitatively same with the plots of $\mathcal{I}_{j\omega_k}$ from Fig. 21 and 23.

On the other hand, when $\Delta E^A = \Delta E^A = \Delta E$ and $d \neq 0$, one gets $P_{A\omega_k} = \mathcal{I}_{A\omega_k}$, $P_{B\omega_k} = \mathcal{I}_{B\omega_k}$, $P_{AB\omega_k} = \mathcal{I}_{AB\omega_k}$ and $P_{\pm\omega_k} = \mathcal{I}_{j\omega_k} \pm |\mathcal{I}_{AB\omega_k}|$. Using these expressions we have obtained the mutual information for $d \neq 0$. We included

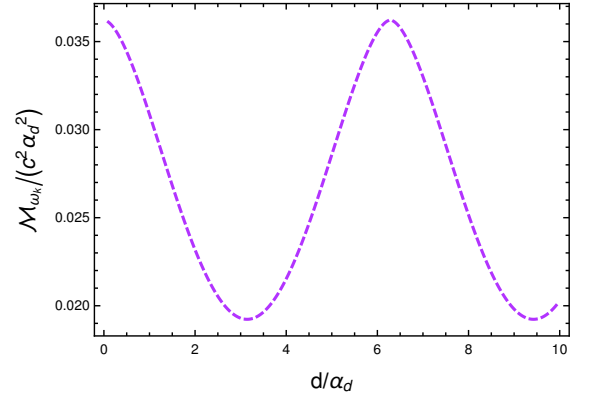


FIG. 38: The mutual information $\mathcal{M}_{\omega_k}(\rho_{AB})/(c^2 r_H^2)$ perceived by two out going null detectors in $(1+3)$ -dimensional de Sitter spacetime corresponding to the conformal vacuum is plotted with respect to the dimensionless parameter d/α_d , for fixed transition frequency $\Delta \bar{E} = \alpha_d \Delta E = 1$, frequency of the field modes $\bar{\omega}_k = \alpha_d \omega_k = 1$, and $\alpha_d k_x = \bar{\omega}_k/2$.

the plots 36 and 37 which represent the change of the mutual information with respect to $\bar{\omega}_k$ and $\Delta \bar{E}$ when $d/\alpha_d = 1$. Qualitatively these plots are not different from the ones with $d/\alpha_d = 0$. Furthermore, unlike the $(1+1)$ dimensional de Sitter case in $(1+3)$ dimensions, the mutual information is dependent, in fact periodically dependent, on d/α_d and this fact is graphically presented in Fig. 38.

IX. DISCUSSION

This work investigates the entanglement harvesting with detectors in outgoing null trajectories from the conformal vacuums in de Sitter and $(1+1)$ dimensional Schwarzschild spacetimes. In particular, we considered the integral representation of Green's functions to estimate the Harvesting conditions corresponding to a specific field mode frequency. We observed that entanglement harvesting is possible, and it is maximum at a particular field mode frequency in the $(1+1)$ dimensional Schwarzschild black hole spacetime with detectors in the same outgoing null trajectory. For this specific trajectory of the same outgoing null path of the two detectors, one observes that $(1+1)$ de Sitter spacetime does not exhibit any entanglement extraction, for the same set of considered parameter values. It signifies that though both detectors are moving along the same outgoing null path in $(1+1)$ de Sitter spacetime, there is no quantum correlation among them. We also observed that these two detectors can be classically correlated as the mutual information between them turned out to be non zero. In contrast, $(1+3)$ dimensional de Sitter spacetime shows entanglement harvesting, for the two detectors in same outgoing null path. When the detectors are in different outgoing null paths, distance d apart, we observed that the concurrence becomes periodic with respect to

the distance d with period and amplitude depending on the field mode frequency. We also observed that the concurrence vanishes at periodic regions and points in d respectively for low and high field mode frequencies in the $(1+1)$ Schwarzschild and $(1+3)$ de Sitter spacetimes. In comparison, in $(1+1)$ dimensional de Sitter spacetime, there are only periodic regions of d with no harvesting. Therefore, concerning the harvested entanglement in terms of the concurrence, one finds the $(1+1)$ dimensional Schwarzschild and $(1+3)$ dimensional de Sitter spacetimes to exhibit qualitatively the same features.

We also observed that in $(1+1)$ dimensional Schwarzschild and $(1+3)$ dimensional de Sitter spacetime, regardless of whether one takes the same or different outgoing null paths, the concurrence continuously decreases with increasing detector transition energy. In $(1+1)$ dimensional de Sitter spacetime and for a certain non-zero value of the distance d , one harvests entanglement in discrete ranges of the detector transition energy, see Fig. 17. In this scenario, we also investigated the role of the vacuum fluctuations of the field in the harvested entanglement.

We observed that the mutual information corresponding to a specific field mode frequency is generally independent of the distance d in $(1+1)$ dimensional Schwarzschild and de Sitter spacetime. In contrast, this mutual information is periodically dependent on d in $(1+3)$ dimensional de Sitter background, but it never becomes zero like the concurrence. This analysis asserts that in these spacetimes, one can obtain certain outgoing null paths for the two detectors where there is no quantum communication between the two detectors. However, classical communication is still possible as perceived through mutual information.

In this analysis we intentionally refrain from making any comment on Hartle-Hawking vacuum for black hole case. This is because we could not properly analyse the related integrals since our choices of regulators could not make the integrals convergent, both at the analytical and numerical levels. One should note that we have specifically considered the outgoing null paths for the detectors. In this regard, one could have considered the ingoing null paths as well. In particular, we have checked the case with both detectors in ingoing null paths corresponding to the Boulware, Unruh, and the Hartle-Hawking vacua. The properties of the entanglement harvesting from the Boulware vacuum, as expected, remain the same like the outgoing scenario. Whereas the ingoing-Unruh situation follows the identical outcome of outgoing-Hartle-Hawking case and therefore we refrain to comment again. Similar situation also arises for ingoing-Hartle-Hawking scenario. Finally, the de-Sitter universe also yields the identical inferences for the ingoing trajectories as the outgoing ones.

We would like to provide a few final comments:

- This article looks for entanglement harvesting from the conformal vacuums with Unruh-DeWitt detec-

tors in null trajectories. We have considered the $(1+1)$ and $(1+3)$ dimensional de Sitter and $(1+1)$ dimensional Schwarzschild backgrounds as they are conformally flat (see [55]). One should notice that the $(1+3)$ dimensional Schwarzschild black hole spacetime is not conformally flat. It is possible to study the effects of quantum field theory in regions near the event horizon and asymptotic infinity in a $(1+3)$ dimensional Schwarzschild background, where the quantum field perceives the effective spacetime to be conformally flat. This effective background does not comply with our current investigation as the null trajectories in our study traverse the whole region outside of the event horizon to spatial infinity. However, the $(1+1)$ dimensional Schwarzschild spacetime is considered a solution of the two-dimensional Einstein-Dilation theory, dimensionally reduced from the Einstein theory (see the discussion above Eq. (17)). Thus our results may retain some signatures of higher dimensions, but we do not have any conclusive evidence at this stage. Therefore, we believe it will be naive to readily comment on the features related to higher dimensional spacetimes just by investigating the same in $(1+1)$ dimensions.

- Note that working with the linear coupling model in $(1+1)$ dimensions has its shortcomings. The presence of infrared (IR) divergence in the position space representation of the Wightman function makes considering the linear coupling model dependent on the IR cutoff in most cases. For instance, one should note that working with linear couplings with detectors switched on for a finite time; one cannot avoid the contributions of the IR cutoff. It compels one to consider the derivative coupling model provided in [77], which gives the Wightman function corresponding to typical Hadamard asymptotics. However, in a few cases, it has been observed that the contributions from the IR cutoff may vanish for infinite switching. The familiar one is the infinite time detector transition probabilities which are free of IR cutoff due to the appearance of Dirac delta distribution with a positive argument (for more examples, see [16]). Moreover, this infinite switching model has also been traditionally considered in various related previous works. In this spirit, we consider the same in our work. In order to circumvent the issues from the IR divergence, we assessed the necessary quantities for fixed field mode frequency (ω_k), giving transition probability corresponding to a specific frequency. Similar attempts have also been taken in [57] to calculate the detector response.
- Here the possibility of entanglement harvesting has been checked through the condition (7). Note that this condition depends on both the local ($\mathcal{I}_{j\omega_k}$) and non-local terms ($\mathcal{I}_{\varepsilon\omega_k}$). This condition says that

the entanglement harvesting is possible only when $|\mathcal{I}_{\varepsilon_{\omega_k}}| - (\mathcal{I}_{A_{\omega_k}} \mathcal{I}_{B_{\omega_k}})^{1/2}$ is positive. Notably, the concurrence, which has been considered here for the measure of entanglement harvesting, depends on the aforesaid difference. Moreover, $\mathcal{I}_{j_{\omega_k}}$ denotes the individual detector transition probability. Therefore, the competition between the non-local terms and the local terms plays a vital role in the measurement of harvesting. In this sense, the perception of the particle by the individual detectors has a significant role in this phenomenon. It should also be noted that the local terms $\mathcal{I}_{j_{\omega_k}}$ denoting individual detector transition probabilities in all of the above cases do not depend on the distance d . Therefore, one concludes that the occurrence of the oscillations in the concurrence with respect to the distance d is due to the nonlocal entangling term $|\mathcal{I}_{\varepsilon_{\omega_k}}|$.

- So far, the examples we have considered in our study are the Schwarzschild background with an event horizon and the de Sitter background without an event horizon. In both cases, we have perceived the occurrence of entanglement harvesting shadow. Now since $(1+1)$ dimensional Schwarzschild background near the event horizon behaves like a Rindler frame, one can expect similar results in the later frame as well. Below we show two such instances of which one will mimic the $(1+1)$ dimensional de Sitter, and the other will mimic the Schwarzschild case.

First, we consider the line element in Rindler coordinates as given by $ds^2 = e^{2a\xi}(-d\eta^2 + d\xi^2)$. In this case, if the Minkowski vacuum is taken as the conformal vacuum, then the null paths $\eta - \xi = d$ followed by detector A and $\eta - \xi = 0$ followed by detector B will provide the necessary integrals for estimating the concurrence. These integrals look similar to those in $(1+1)$ de Sitter spacetime. Therefore one could expect similar features in concurrence.

Second, we consider the line element in Rindler coordinates as given by $ds^2 = -2ax dt^2 + dx^2/(2ax)$, which is reminiscent of the near horizon $(1+1)$ dimensional Schwarzschild spacetime. Here one can construct a tortoise-like coordinate ($dx_\star = dx/(2ax)$) transformation which makes the metric conformally flat. In these coordinates (t, x_\star) , the defined vacuum for the fields will be identical to the Boulware vacuum. Therefore we consider our detectors to be moving in null paths in the Eddington-Finkelstein-like coordinates for the Rindler one; then, the situation will be quite identical to the already obtained results for the $(1+1)$ Schwarzschild background.

It may be interesting to note that the entanglement shadow regions occur for both the black hole and the de Sitter spacetimes. Also, we found that the same can occur for the Rindler spacetime as well.

A few things can be noted related to these examples, like de Sitter universe does not contain an event horizon, whereas Rindler spacetime is curvature less. Therefore the appearance of the entanglement shadow might be dependent on the choices of our paths and the background field vacua.

- In $(1+1)$ dimensional de Sitter background, we have observed that with increasing field mode frequency $\bar{\omega}_k$ the length of the shadow region decreases. Moreover, for a finite value of $\bar{\omega}_k$ (in a range $\bar{\omega}_k \in [10^{-4}, 10^4]$) the lower kinks in the curves remain below the zero concurrence line. Therefore, in this case, we always have shadow regions. Hence, one cannot find a parameter space for which entanglement harvesting is always or never possible. In the $(1+1)$ Schwarzschild and $(1+3)$ de Sitter background spacetimes, we found that it is not always point-like entanglement shadows. The occurrence of entanglement harvesting shadow regions is possible in relatively low frequency $\bar{\omega}_k$ regimes. With increasing $\bar{\omega}_k$, these shadow regions decrease and become shadow points. However, increasing the frequency further does not make these shadow points go away, i.e., we keep getting entanglement harvesting shadow points for larger and larger $\bar{\omega}_k$ values. In this regard, we have considered the frequency range up to 10^4 . However, the similarity between $(1+1)$ Schwarzschild and $(1+3)$ de Sitter may occur in different frequency ranges.

The above observations show that $(1+1)$ dimensional Schwarzschild and $(1+3)$ dimensional de Sitter backgrounds have a close resemblance between them in terms of the shadows. In contrast, the $(1+1)$ dimensional de Sitter case does not show such similarity. The possible reason behind this may be as follows. Note that the concurrence is dependent on both the non-local entangling term $\mathcal{I}_{\varepsilon_{\omega_k}}$ and the local term $\mathcal{I}_{j_{\omega_k}}$. Therefore, the shadow happens only if $\sqrt{\mathcal{I}_{A_{\omega_k}} \mathcal{I}_{B_{\omega_k}}} \geq |\mathcal{I}_{\varepsilon_{\omega_k}}|$. Interestingly, in $(1+1)$ dimensional de Sitter case $\mathcal{I}_{j_{\omega_k}}$ are independent of ω_k , see Eq. (63). While in the other two spacetimes, the same is ω_k dependent, see Eqs. (46) and (71). It implies that the subtracted term $\sqrt{\mathcal{I}_{A_{\omega_k}} \mathcal{I}_{B_{\omega_k}}}$ in the concurrence changes for $(1+1)$ Schwarzschild and $(1+3)$ de Sitter cases as one changes ω_k . On the other hand, for the $(1+1)$ de Sitter case, the same does not happen. Hence, it may be the reason that in the first scenario, we have a change in shadow from regions to points as one increases $\bar{\omega}_k$. Since this ω_k is a property of the field, the above two scenarios mostly depend on the particular field mode with which the detectors are interacting. Therefore, we feel that these observations are based on the underlying properties of the quantum fields rather than the background geometry. Of course, further investigation is needed to provide a concrete reason in favour of the above

scenarios. Also, it would be interesting to provide a detailed analysis in finding a condition that will dictate the critical value of $\bar{\omega}_k$ above which the shadow region becomes a point.

Acknowledgments

SB would like to thank the Indian Institute of Technology Guwahati (IIT Guwahati) for financial support. DB would like to acknowledge Ministry of Education, Government of India for providing financial support for his research via the PMRF May 2021 scheme. The research of BRM is partially supported by a START-UP RESEARCH GRANT (No. SG/PHY/P/BRM/01) from the Indian Institute of Technology Guwahati, India. We thank the anonymous referee for the crucial suggestions that have helped to improve the manuscript.

to two detectors in outgoing null trajectories in an (1 + 1) dimensional Schwarzschild black hole spacetime. In particular, this integral is evaluated as

$$\mathcal{I}_{\varepsilon\omega_k}^W = \frac{e^{id\omega_k} (4r_H^2\omega_k^2 + 9\epsilon^2)}{r_H^2 (4\omega_k^2 - \Delta E^2) - 2i\Delta E r_H \epsilon + \epsilon^2} \frac{(\epsilon + ir_H(2\omega_k - \Delta E))^{-\epsilon+2ir_H(\omega_k-\Delta E)} (\epsilon - ir_H(\Delta E + 2\omega_k))^{-\epsilon-2ir_H(\Delta E+\omega_k)}}{\Gamma(\epsilon - 2ir_H(\omega_k - \Delta E))\Gamma(2ir_H(\omega_k + \Delta E) + \epsilon)} . \quad (A1)$$

Appendix A: Evaluation of the integrals $\mathcal{I}_{\varepsilon\omega_k}^W$ and $\mathcal{I}_{\varepsilon\omega_k}^R$ in Schwarzschild black hole spacetime

1. Boulware vacuum

We introduce regulator of the form $(y_A y_B)^\epsilon e^{-\epsilon(y_A+y_B)}$ to evaluate the integral $\mathcal{I}_{\varepsilon\omega_k}^W$ from Eq. (51) corresponding

On the other hand, using same regulator of the form $(z_A z_B)^\epsilon e^{-\epsilon(z_A+z_B)}$ with small positive real parameter ϵ the integral $\mathcal{I}_{\varepsilon\omega_k}^R$ from Eq. (54) is evaluated as

$$\begin{aligned} \mathcal{I}_{\varepsilon\omega_k}^R = & -\frac{e^{-id\omega_k} (-1 + e^{2id\omega_k})}{(4\omega_k^2 - \Delta E^2)r_H^2 - 2i\Delta E r_H \epsilon + \epsilon^2} (ir_H(2\omega_k - \Delta E) + \epsilon)^{2ir_H(\omega_k-\Delta E)-\epsilon} (\epsilon - ir_H(2\omega_k + \Delta E))^{-2ir_H(\omega_k+\Delta E)-\epsilon} \\ & \times (4r_H^2\omega_k^2 + 9\epsilon^2) \Gamma(\epsilon - 2ir_H(\omega_k - \Delta E)) \Gamma(2ir_H(\omega_k + \Delta E) + \epsilon) \\ & + \left[-\frac{4ie^{id\omega_k} (ir_H(2\omega_k - \Delta E) + \epsilon)^{-2(2ir_H\Delta E+\epsilon)}}{2r_H(\omega_k + \Delta E) - i\epsilon} \right. \\ & \times {}_2F_1 \left(2(2ir_H\Delta E + \epsilon), 2ir_H(\omega_k + \Delta E) + \epsilon; 2ir_H(\omega_k + \Delta E) + \epsilon + 1; \frac{2r_H\omega_k + r_H\Delta E + i\epsilon}{2r_H\omega_k - r_H\Delta E - i\epsilon} \right) \\ & + \frac{4e^{-id\omega_k} (2ir_H\Delta E + \epsilon)(\epsilon - ir_H(2\omega_k + \Delta E))^{-2(2ir_H\Delta E+\epsilon)}}{(2r_H(\omega_k - \Delta E) + i\epsilon)(r_H(2\omega_k + \Delta E) + i\epsilon)} \\ & \times {}_2F_1 \left(\epsilon - 2ir_H(\omega_k - \Delta E), 4ir_H\Delta E + 2\epsilon + 1; -2ir_H(\omega_k - \Delta E) + \epsilon + 1; \frac{2r_H\omega_k - r_H\Delta E - i\epsilon}{2r_H\omega_k + r_H\Delta E + i\epsilon} \right) \\ & - \frac{4e^{-id\omega_k} (2ir_H\Delta E + \epsilon)(\epsilon - ir_H(2\omega_k + \Delta E))^{-4ir_H\Delta E-2\epsilon-1}}{-2ir_H(\omega_k - \Delta E) + \epsilon + 1} \\ & \times {}_2F_1 \left(-2ir_H(\omega_k - \Delta E) + \epsilon + 1, 4ir_H\Delta E + 2\epsilon + 1; -2ir_H(\omega_k - \Delta E) + \epsilon + 2; \frac{2r_H\omega_k - r_H\Delta E - i\epsilon}{2r_H\omega_k + r_H\Delta E + i\epsilon} \right) \\ & - \frac{2e^{id\omega_k} (2r_H\Delta E - i\epsilon)(ir_H(2\omega_k - \Delta E) + \epsilon)^{-4ir_H\Delta E-2(\epsilon+1)} (4r_H\Delta E - i(2\epsilon+1))}{2ir_H(\omega_k + \Delta E) + \epsilon + 1} \\ & \times {}_2F_1 \left(2(2ir_H\Delta E + \epsilon + 1), 2ir_H(\omega_k + \Delta E) + \epsilon + 1; 2ir_H(\omega_k + \Delta E) + \epsilon + 2; \frac{2r_H\omega_k + r_H\Delta E + i\epsilon}{2r_H\omega_k - r_H\Delta E - i\epsilon} \right) \\ & - \frac{4ie^{id\omega_k} (ir_H(2\omega_k - \Delta E) + \epsilon)^{-4ir_H\Delta E-2\epsilon-1} (2ir_H\Delta E + \epsilon)}{2r_H(\omega_k + \Delta E) - i\epsilon} \end{aligned}$$

$$\begin{aligned}
& \times {}_2F_1 \left(2ir_H(\omega_k + \Delta E) + \epsilon, 4ir_H\Delta E + 2\epsilon + 1; 2ir_H(\omega_k + \Delta E) + \epsilon + 1; \frac{2r_H\omega_k + r_H\Delta E + i\epsilon}{2r_H\omega_k - r_H\Delta E - i\epsilon} \right) \\
& + \frac{4e^{id\omega_k}(ir_H(2\omega_k - \Delta E) + \epsilon)^{-4ir_H\Delta E - 2\epsilon - 1}(2ir_H\Delta E + \epsilon)}{2ir_H(\omega_k + \Delta E) + \epsilon + 1} \\
& \times {}_2F_1 \left(2ir_H(\omega_k + \Delta E) + \epsilon + 1, 4ir_H\Delta E + 2\epsilon + 1; 2ir_H(\omega_k + \Delta E) + \epsilon + 2; \frac{2r_H\omega_k + r_H\Delta E + i\epsilon}{2r_H\omega_k - r_H\Delta E - i\epsilon} \right) \\
& + \frac{8i(\epsilon - ir_H\Delta E)^{-4ir_H\Delta E - 2\epsilon} {}_2F_1(2ir_H\Delta E + \epsilon, 2(2ir_H\Delta E + \epsilon); 2ir_H\Delta E + \epsilon + 1; -1) \sin(d\omega_k)}{2ir_H\Delta E + \epsilon} \\
& + \frac{8i(\epsilon - ir_H\Delta E)^{-4ir_H\Delta E - 2\epsilon - 1}(2ir_H\Delta E + \epsilon) \sin(d\omega_k)}{2ir_H\Delta E + \epsilon + 1} \\
& \times {}_2F_1(2ir_H\Delta E + \epsilon + 1, 4ir_H\Delta E + 2\epsilon + 1; 2ir_H\Delta E + \epsilon + 2; -1) \\
& + \frac{4(2r_H\Delta E - i\epsilon)(\epsilon - ir_H\Delta E)^{-4ir_H\Delta E - 2\epsilon - 1}(4r_H\Delta E - i(2\epsilon + 1)) \sin(d\omega_k)}{(r_H\Delta E + i\epsilon)(2ir_H\Delta E + \epsilon + 1)} \\
& \times {}_2F_1(2ir_H\Delta E + \epsilon + 1, 2(2ir_H\Delta E + \epsilon + 1); 2ir_H\Delta E + \epsilon + 2; -1) \\
& - \frac{4e^{-id\omega_k}(\epsilon - ir_H(2\omega_k + \Delta E))^{-4ir_H\Delta E - 2\epsilon}}{\epsilon - 2ir_H(\omega_k - \Delta E)} \\
& \times {}_2F_1 \left(\epsilon - 2ir_H(\omega_k - \Delta E), 2(2ir_H\Delta E + \epsilon); -2ir_H(\omega_k - \Delta E) + \epsilon + 1; \frac{2r_H\omega_k - r_H\Delta E - i\epsilon}{2r_H\omega_k + r_H\Delta E + i\epsilon} \right) \\
& - \frac{2e^{-id\omega_k}(2r_H\Delta E - i\epsilon)(\epsilon - ir_H(2\omega_k + \Delta E))^{-2(2ir_H\Delta E + \epsilon)}(4r_H\Delta E - i(2\epsilon + 1))}{(r_H(2\omega_k + \Delta E) + i\epsilon)^2(-2ir_H(\omega_k - \Delta E) + \epsilon + 1)} \\
& \times {}_2F_1 \left(-2ir_H(\omega_k - \Delta E) + \epsilon + 1, 2(2ir_H\Delta E + \epsilon + 1); -2ir_H(\omega_k - \Delta E) + \epsilon + 2; \frac{2r_H\omega_k - r_H\Delta E - i\epsilon}{2r_H\omega_k + r_H\Delta E + i\epsilon} \right) \\
& - \frac{8(\epsilon - ir_H\Delta E)^{-2(2ir_H\Delta E + \epsilon)} {}_2F_1(2ir_H\Delta E + \epsilon, 4ir_H\Delta E + 2\epsilon + 1; 2ir_H\Delta E + \epsilon + 1; -1) \sin(d\omega_k)}{r_H\Delta E + i\epsilon} \Big] \Gamma(4ir_H\Delta E + 2\epsilon) \\
& + \frac{2(\epsilon - ir_H\Delta E)^{-2(2ir_H\Delta E + \epsilon)} (-8ir_H^2\Delta E^2 + 4r_H\epsilon\Delta E + 5i\epsilon^2) \Gamma(2ir_H\Delta E + \epsilon)^2 \sin(d\omega_k)}{(r_H\Delta E + i\epsilon)^2} \\
& + \frac{8(\epsilon - ir_H\Delta E)^{-2(2ir_H\Delta E + \epsilon)} \Gamma(2ir_H\Delta E + \epsilon) \Gamma(2ir_H\Delta E + \epsilon + 1) \sin(d\omega_k)}{r_H\Delta E + i\epsilon}. \tag{A2}
\end{aligned}$$

For both $\mathcal{I}_{\epsilon\omega_k}^W$ and $\mathcal{I}_{\epsilon\omega_k}^R$ we have considered the evaluation for $\Delta E^A = \Delta E^B = \Delta E$. Here the functions $\Gamma(x)$ and ${}_2F_1(x)$ respectively denote the *Gamma functions* and the *Hypergeometric functions*.

2. Unruh vacuum

One can introduce regulator of the form $(y_A y_B)^\epsilon e^{-\epsilon(y_A + y_B)}$ to evaluate the integral $\mathcal{I}_{\epsilon\omega_k}^W$ from Eq. (57) corresponding to detectors in outgoing null trajectories in an (1 + 1) dimensional Schwarzschild black hole spacetime with Unruh vacuum. In particular, this integral has the same expression as provided in Eq. (A1).

On the other hand, utilizing the same regulator of the form $(y_A y_B)^\epsilon e^{-\epsilon(y_A + y_B)}$ one can also proceed to evaluate

the integral $\mathcal{I}_{\epsilon\omega_k}^R$ from Eq. (58). In particular, one can observe that this integral is different from Eq. (53) of the Boulware case in only the last term with a factor of $-2i \sin\{\omega_k 2r_H(1 - \exp(-d/2r_H))\}$. Let us term this quantity to be $\mathcal{I}_{\epsilon\omega_k}^{\mathcal{E}}$ and evaluate this integral

$$\begin{aligned}
\mathcal{I}_{\epsilon\omega_k}^{\mathcal{E}} &= -2i \sin\left\{\omega_k 2r_H(1 - e^{-d/2r_H})\right\} \int_{r_H}^{\infty} dr_A \frac{r_A + r_H}{r_A - r_H} \\
&\times \int_{r_H}^{r_A} dr_B \frac{r_B + r_H}{r_B - r_H} e^{i\{\Delta E^B r_B + \Delta E^A(r_A + d)\}} \\
&\times \left(\frac{r_B}{r_H} - 1\right)^{2ir_H\Delta E^B} \left(\frac{r_A}{r_H} - 1\right)^{2ir_H\Delta E^A}. \tag{A3}
\end{aligned}$$

This integral can be evaluated with regulator $(y_A y_B)^\epsilon e^{-\epsilon(y_A + y_B)}$ and is obtained as

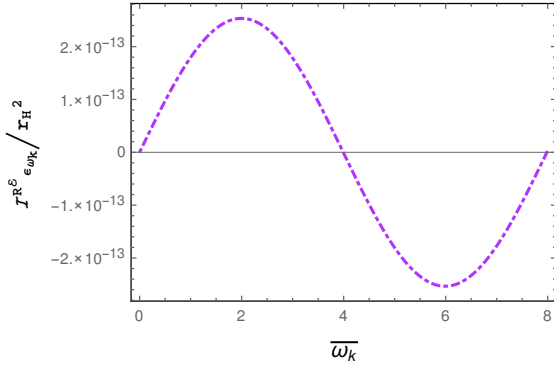


FIG. 39: The quantity $\mathcal{I}_{\epsilon\omega_k}^{R\epsilon}$ is plotted with respect to $\bar{\omega}_k$ for fixed $d/r_H = 1$, $\Delta E = 1$.

$$\begin{aligned}
\mathcal{I}_{\epsilon\omega_k}^{R\epsilon} = & -2 \sin \left\{ \omega_k 2r_H (1 - e^{-d/2r_H}) \right\} (\epsilon - i\Delta E r_H)^{-4i\Delta E r_H - 2\epsilon - 1} \\
& \left[2 \left\{ - \frac{2(\Delta E r_H + i\epsilon) {}_2F_1(2ir_H \Delta E + \epsilon, 2(2ir_H \Delta E + \epsilon); 2ir_H \Delta E + \epsilon + 1; -1)}{\epsilon + 2i\Delta E r_H} \right. \right. \\
& - 2i {}_2F_1(2ir_H \Delta E + \epsilon, 4ir_H \Delta E + 2\epsilon + 1; 2ir_H \Delta E + \epsilon + 1; -1) \\
& + \frac{(4i\Delta E r_H + 2\epsilon + 1)(2\Delta E r_H - i\epsilon) {}_2F_1(2ir_H \Delta E + \epsilon + 1, 2(2ir_H \Delta E + \epsilon + 1); 2ir_H \Delta E + \epsilon + 2; -1)}{(\Delta E r_H + i\epsilon)(2\Delta E r_H - i(\epsilon + 1))} \\
& \left. \left. - \frac{2i(2\Delta E r_H - i\epsilon) {}_2F_1(2ir_H \Delta E + \epsilon + 1, 4ir_H \Delta E + 2\epsilon + 1; 2ir_H \Delta E + \epsilon + 2; -1)}{2\Delta E r_H - i(\epsilon + 1)} \right\} \Gamma(4ir_H \Delta E + 2\epsilon) \right. \\
& \left. + \frac{(8\Delta E^2 r_H^2 + 4i\Delta E r_H \epsilon - 5\epsilon^2) \Gamma(2ir_H \Delta E + \epsilon)^2}{\Delta E r_H + i\epsilon} + 4i\Gamma(2ir_H \Delta E + \epsilon + 1)\Gamma(2ir_H \Delta E + \epsilon) \right]. \quad (\text{A4})
\end{aligned}$$

One can numerically plot this quantity for similar parameter values for which the plots of $\mathcal{I}_{\epsilon\omega_k}^R$ are performed and observe that $\mathcal{I}_{\epsilon\omega_k}^{R\epsilon}$ is many order lower, see. Fig. 39.

Appendix B: Heaviside step function corresponding to the Unruh modes

The Kruskal null coordinates (V, U) are related to the null coordinates (v, u) by the relation $V = 2r_H e^{v/2r_H}$ and $U = -2r_H e^{-u/2r_H}$. Whereas these coordinates (v, u) are again related to the Schwarzschild time and the tortoise coordinates as $v = t_s + r_*$ and $u = t_s - r_*$. We have already stated that while dealing with modes represented in terms of the Kruskal coordinates one should consider the Kruskal time $T_K = (U + V)/2$. This time is represented in terms of the Schwarzschild time and the tortoise coordinates as $T_K = 2r_H e^{r_*/2r_H} \sinh(t_s/2r_H)$. We have considered that Alice and Bob denoted respectively by the detectors A and B are both moving along outgoing null trajectories. However, for Alice the outgoing null path is $t_{sA} - r_{*A} = d$, while for Bob the path is $t_{sB} - r_{*B} = 0$. With these conditions let us search for the

situation when the Heaviside step function $\theta(T_{KA} - T_{KB})$ will be non zero.

For the above mentioned Heaviside step function to be non zero one must have $T_{KA} \geq T_{KB}$. In terms of the Schwarzschild time and the tortoise coordinate and using the appropriate prescription of the null paths for the detectors A and B this condition becomes

$$e^{(2r_{*A}+d)/2r_H} - e^{r_{*B}/r_H} \geq e^{-d/2r_H} - 1. \quad (\text{B1})$$

Here we have considered d to be positive and real. In that case the maximum value of the right hand side of the above inequality is zero and therefore the above will be automatically satisfied if one has

$$e^{(2r_{*A}+d)/2r_H} - e^{r_{*B}/r_H} \geq 0. \quad (\text{B2})$$

This can be re-expressed as $e^{(r_{*A}-r_{*B})/r_H} \geq e^{-(d/2r_H)}$. Now again as $0 \leq e^{-(d/2r_H)} \leq 1$, the required condition will be satisfied if one has

$$e^{(r_{*A}-r_{*B})/r_H} \geq 1. \quad (\text{B3})$$

This basically implies that one must have $r_{*A} \geq r_{*B}$ or $r_A \geq r_B$. Note that this very condition has been considered in our main analysis.

Appendix C: Evaluation of the integrals $\mathcal{I}_{\varepsilon\omega_k}^W$ and $\mathcal{I}_{\varepsilon\omega_k}^R$ in de Sitter spacetime

1. (1+1) dimensions

With the introduction of regulator of the form $(z_A z_B)^\epsilon e^{-\epsilon(z_A+z_B)}$ the integral $\mathcal{I}_{\varepsilon\omega_k}^W$ from Eq. (66) corresponding to two detectors in outgoing null trajectories in an (1+1) dimensional de Sitter spacetime can be eval-

uated to be

$$\mathcal{I}_{\varepsilon\omega_k}^W = e^{-id\omega_k} \Gamma(\epsilon - i\alpha_d \Delta E)^2 (\epsilon - 2i\alpha_d \omega_k)^{-\epsilon + i\alpha_d \Delta E} \times (\epsilon + 2i\alpha_d \omega_k)^{-\epsilon + i\alpha_d \Delta E}. \quad (C1)$$

On the other hand, using same regulator of the form $(z_A z_B)^\epsilon e^{-\epsilon(z_A+z_B)}$ with small positive real parameter ϵ the integral $\mathcal{I}_{\varepsilon\omega_k}^R$ from Eq. (67) is evaluated as

$$\begin{aligned} \mathcal{I}_{\varepsilon\omega_k}^R = & \Gamma(\epsilon - i\alpha_d \Delta E) \left[\Gamma(2\epsilon - 2i\alpha_d \Delta E) \left\{ e^{id\omega_k} (\epsilon + 2i\alpha_d \omega_k)^{-2\epsilon + 2i\alpha_d \Delta E} \right. \right. \\ & {}_2\tilde{F}_1 \left(\epsilon - i\alpha_d \Delta E, 2(\epsilon - i\alpha_d \Delta E); -i\alpha_d \Delta E + \epsilon + 1; \frac{4i\omega_k \alpha_d}{2i\omega_k \alpha_d + \epsilon} - 1 \right) - e^{-id\omega_k} (\epsilon - 2i\alpha_d \omega_k)^{-2\epsilon + 2i\alpha_d \Delta E} \\ & \left. {}_2\tilde{F}_1 \left(\epsilon - i\alpha_d \Delta E, 2(\epsilon - i\alpha_d \Delta E); -i\alpha_d \Delta E + \epsilon + 1; \frac{4\omega_k \alpha_d}{2\omega_k \alpha_d + i\epsilon} - 1 \right) \right\} - i\epsilon^{-2\epsilon + 2i\alpha_d \Delta E} \sin(d\omega_k) \Gamma(\epsilon - i\alpha_d \Delta E) \Big]. \end{aligned} \quad (C2)$$

For both $\mathcal{I}_{\varepsilon\omega_k}^W$ and $\mathcal{I}_{\varepsilon\omega_k}^R$ we have considered the evaluation for $\Delta E^A = \Delta E^B = \Delta E$. Here the functions $\Gamma(x)$ and ${}_2\tilde{F}_1(x)$ respectively denote the *Gamma functions* and the *regularized Hypergeometric functions*.

2. (1+3) dimensions

With the introduction of regulator of the form $(z_A z_B)^\epsilon e^{-\epsilon(z_A+z_B)}$ the integral $\mathcal{I}_{\varepsilon\omega_k}^W$ from Eq. (74) corresponding to two detectors in outgoing null trajectories in an (1+3) dimensional de Sitter spacetime can be eval-

uated to be

$$\begin{aligned} \mathcal{I}_{\varepsilon\omega_k}^W = & e^{-idk_x} \Gamma(-i\alpha_d \Delta E + \epsilon + 1)^2 \\ & \times (\epsilon - i\alpha_d(k_x + \omega_k))^{i\alpha_d \Delta E - \epsilon - 1} \\ & (\epsilon + i\alpha_d(k_x + \omega_k))^{i\alpha_d \Delta E - \epsilon - 1} + e^{idk_x} \Gamma(-i\alpha_d \Delta E + \epsilon + 1)^2 \\ & (\epsilon - i\alpha_d(k_x - \omega_k))^{i\alpha_d \Delta E - \epsilon - 1} (i\alpha_d k_x - i\alpha_d \omega_k + \epsilon)^{i\alpha_d \Delta E - \epsilon - 1}. \end{aligned} \quad (C3)$$

On the other hand, using same regulator of the form $(z_A z_B)^\epsilon e^{-\epsilon(z_A+z_B)}$ with small positive real parameter ϵ the integral $\mathcal{I}_{\varepsilon\omega_k}^R$ from Eq. (75) is evaluated as

$$\begin{aligned} \mathcal{I}_{\varepsilon\omega_k}^R = & \frac{e^{-idk_x}}{-i\alpha_d \Delta E + \epsilon + 1} \Gamma(-2i\alpha_d \Delta E + 2\epsilon + 2) \left[(\epsilon - i\alpha_d(k_x - \omega_k))^{-2(\epsilon+1)+2i\alpha_d \Delta E} \right. \\ & \times {}_2F_1 \left(-i\alpha_d \Delta E + \epsilon + 1, -2i\alpha_d \Delta E + 2\epsilon + 2; -i\alpha_d \Delta E + \epsilon + 2; \frac{k_x \alpha_d - \omega_k \alpha_d - i\epsilon}{k_x \alpha_d - \omega_k \alpha_d + i\epsilon} \right) \\ & - e^{2idk_x} (\epsilon + i\alpha_d(k_x - \omega_k))^{-2(\epsilon+1)+2i\alpha_d \Delta E} \\ & \left. \times {}_2F_1 \left(-i\alpha_d \Delta E + \epsilon + 1, -2i\alpha_d \Delta E + 2\epsilon + 2; -i\alpha_d \Delta E + \epsilon + 2; \frac{k_x \alpha_d - \omega_k \alpha_d + i\epsilon}{k_x \alpha_d - \omega_k \alpha_d - i\epsilon} \right) \right] \\ & + e^{-idk_x} \Gamma(-i\alpha_d \Delta E + \epsilon + 1) \Gamma(-2i\alpha_d \Delta E + 2\epsilon + 2) \left[e^{2idk_x} (\epsilon + i\alpha_d(k_x + \omega_k))^{-2(\epsilon+1)+2i\alpha_d \Delta E} \right. \\ & \times {}_2\tilde{F}_1 \left(-i\alpha_d \Delta E + \epsilon + 1, 2(-i\alpha_d \Delta E + \epsilon + 1); -i\alpha_d \Delta E + \epsilon + 2; \frac{(k_x + \omega_k) \alpha_d + i\epsilon}{(k_x + \omega_k) \alpha_d - i\epsilon} \right) \\ & \left. - (\epsilon - i\alpha_d(k_x + \omega_k))^{-2(\epsilon+1)+2i\alpha_d \Delta E} \right] \end{aligned}$$

$$\times {}_2\tilde{F}_1\left(-i\alpha_d\Delta E + \epsilon + 1, 2(-i\alpha_d\Delta E + \epsilon + 1); -i\alpha_d\Delta E + \epsilon + 2; \frac{(k_x + \omega_k)\alpha_d - i\epsilon}{(k_x + \omega_k)\alpha_d + i\epsilon}\right). \quad (C4)$$

Here also we have considered the specific scenario $\Delta E^A = \Delta E^B = \Delta E$ for evaluating both $\mathcal{I}_{\varepsilon\omega_k}^W$ and $\mathcal{I}_{\varepsilon\omega_k}^R$, and the functions $\Gamma(x)$, ${}_2F_1(x)$ and ${}_2\tilde{F}_1(x)$ respectively denote

the *Gamma functions*, the *Hypergeometric functions*, and the *regularized Hypergeometric functions*.

-
- [1] B. Reznik, Found. Phys. **33**, 167 (2003), arXiv:quant-ph/0212044.
 - [2] S.-Y. Lin and B. Hu, Phys. Rev. D **81**, 045019 (2010), arXiv:0910.5858.
 - [3] J. L. Ball, I. Fuentes-Schuller, and F. P. Schuller, Phys. Lett. A **359**, 550 (2006), arXiv:quant-ph/0506113.
 - [4] M. Cliche and A. Kempf, Phys. Rev. A **81**, 012330 (2010), arXiv:0908.3144.
 - [5] E. Martin-Martinez and N. C. Menicucci, Class. Quant. Grav. **29**, 224003 (2012), arXiv:1204.4918.
 - [6] G. Salton, R. B. Mann, and N. C. Menicucci, New J. Phys. **17**, 035001 (2015), arXiv:1408.1395.
 - [7] E. Martin-Martinez, A. R. H. Smith, and D. R. Terno, Phys. Rev. D **93**, 044001 (2016), arXiv:1507.02688.
 - [8] H. Cai and Z. Ren, Sci. Rep. **8**, 11802 (2018).
 - [9] G. Menezes, Phys. Rev. **D97**, 085021 (2018), arXiv:1712.07151.
 - [10] G. Menezes, N. Svaiter, and C. Zarro, Phys. Rev. A **96**, 062119 (2017), arXiv:1709.08702.
 - [11] W. Zhou and H. Yu, Phys. Rev. D **96**, 045018 (2017).
 - [12] F. Benatti and R. Floreanini, Phys. Rev. A **70**, 012112 (2004).
 - [13] Y. Pan and B. Zhang, Phys. Rev. A **101**, 062111 (2020), arXiv:2009.05179.
 - [14] G. Menezes, Phys. Rev. **D94**, 105008 (2016), arXiv:1512.03636.
 - [15] W. Cong, C. Qian, M. R. R. Good, and R. B. Mann, JHEP **10**, 067 (2020), arXiv:2006.01720.
 - [16] P. Chowdhury and B. R. Majhi, JHEP **05**, 025 (2022), 2110.11260.
 - [17] G. R. Kane and B. R. Majhi, Phys. Rev. D **104**, 041701 (2021), arXiv:2105.11709.
 - [18] D. Barman and B. R. Majhi, JHEP **05**, 046 (2022), 2111.00711.
 - [19] I. Fuentes-Schuller and R. B. Mann, Phys. Rev. Lett. **95**, 120404 (2005), arXiv:quant-ph/0410172.
 - [20] J. Hu and H. Yu, Phys. Rev. A **91**, 012327 (2015), arXiv:1501.03321.
 - [21] S. Barman and B. R. Majhi, JHEP **03**, 245 (2021), arXiv:2101.08186.
 - [22] S. J. Summers and R. Werner, Physics Letters A **110**, 257 (1985), ISSN 0375-9601.
 - [23] S. J. Summers and R. Werner, Journal of Mathematical Physics **28**, 2440 (1987), <https://doi.org/10.1063/1.527733>.
 - [24] A. Valentini, Physics Letters A **153**, 321 (1991), ISSN 0375-9601.
 - [25] B. Reznik, A. Retzker, and J. Silman, Phys. Rev. A **71**, 042104 (2005), arXiv:quant-ph/0310058.
 - [26] L. J. Henderson, R. A. Hennigar, R. B. Mann, A. R. Smith, and J. Zhang, Class. Quant. Grav. **35**, 21LT02 (2018), arXiv:1712.10018.
 - [27] L. J. Henderson and N. C. Menicucci, Phys. Rev. D **102**, 125026 (2020), arXiv:2005.05330.
 - [28] N. Stritzelberger, L. J. Henderson, V. Baccetti, N. C. Menicucci, and A. Kempf (2020), arXiv:2006.11291.
 - [29] M. Hotta, Phys. Rev. D **78**, 045006 (2008), arXiv:0803.2272.
 - [30] M. Hotta, Journal of the Physical Society of Japan **78**, 034001 (2009).
 - [31] M. Frey, K. Funo, and M. Hotta, Phys. Rev. E **90**, 012127 (2014).
 - [32] G. L. Ver Steeg and N. C. Menicucci, Phys. Rev. D **79**, 044027 (2009), arXiv:0711.3066.
 - [33] A. Pozas-Kerstjens and E. Martin-Martinez, Phys. Rev. D **92**, 064042 (2015), arXiv:1506.03081.
 - [34] S. Kukita and Y. Nambu, Entropy **19**, 449 (2017), arXiv:1708.01359.
 - [35] A. Pozas-Kerstjens and E. Martin-Martinez, Phys. Rev. D **94**, 064074 (2016), arXiv:1605.07180.
 - [36] E. Martín-Martínez, E. G. Brown, W. Donnelly, and A. Kempf, Phys. Rev. A **88**, 052310 (2013), arXiv:1309.1090.
 - [37] K. Lorek, D. Pecak, E. G. Brown, and A. Dragan, Phys. Rev. A **90**, 032316 (2014), arXiv:1405.4449.
 - [38] E. G. Brown, W. Donnelly, A. Kempf, R. B. Mann, E. Martin-Martinez, and N. C. Menicucci, New J. Phys. **16**, 105020 (2014), arXiv:1407.0071.
 - [39] A. Sachs, R. B. Mann, and E. Martin-Martinez, Phys. Rev. D **96**, 085012 (2017), arXiv:1704.08263.
 - [40] J. Trevison, K. Yamaguchi, and M. Hotta, J. Phys. A **52**, 125402 (2019), arXiv:1807.03467.
 - [41] T. Li, B. Zhang, and L. You, Phys. Rev. D **97**, 045005 (2018), arXiv:1802.07886.
 - [42] A. Peres, Phys. Rev. Lett. **77**, 1413 (1996), arXiv:quant-ph/9604005.
 - [43] M. Horodecki, P. Horodecki, and R. Horodecki, Phys. Lett. A **223**, 1 (1996), arXiv:quant-ph/9605038.
 - [44] J.-I. Koga, G. Kimura, and K. Maeda, Phys. Rev. A **97**, 062338 (2018), arXiv:1804.01183.
 - [45] K. K. Ng, R. B. Mann, and E. Martín-Martínez, Phys. Rev. D **97**, 125011 (2018), arXiv:1805.01096.
 - [46] J.-i. Koga, K. Maeda, and G. Kimura, Phys. Rev. D **100**, 065013 (2019), arXiv:1906.02843.
 - [47] E. Tjoa and R. B. Mann, JHEP **08**, 155 (2020), arXiv:2007.02955.
 - [48] J. Foo, R. B. Mann, and M. Zych, Phys. Rev. D **103**, 065013 (2021), arXiv:2101.01912.
 - [49] K. Gallock-Yoshimura, E. Tjoa, and R. B. Mann, Phys. Rev. D **104**, 025001 (2021), 2102.09573.

- [50] L. J. Henderson, R. A. Hennigar, R. B. Mann, A. R. H. Smith, and J. Zhang, JHEP **05**, 178 (2019), arXiv:1809.06862.
- [51] K. K. Ng, R. B. Mann, and E. Martín-Martínez, Phys. Rev. D **98**, 125005 (2018), arXiv:1809.06878.
- [52] W. Cong, E. Tjoa, and R. B. Mann, JHEP **06**, 021 (2019), [Erratum: JHEP **07**, 051 (2019)], arXiv:1810.07359.
- [53] D. Barman, S. Barman, and B. R. Majhi, JHEP **07**, 124 (2021), arXiv:2104.11269.
- [54] M. P. G. Robbins, L. J. Henderson, and R. B. Mann, Class. Quant. Grav. **39**, 02LT01 (2022), 2010.14517.
- [55] N. D. Birrell and P. C. W. Davies, *Quantum fields in curved space*, Cambridge Monographs on Mathematical Physics (Cambridge University Press, 1984).
- [56] A. Das, S. Dalui, C. Chowdhury, and B. R. Majhi, Phys. Rev. D **100**, 085002 (2019), arXiv:1902.03735.
- [57] M. O. Scully, S. Fulling, D. Lee, D. N. Page, W. Schleich, and A. Svidzinsky, Proc. Nat. Acad. Sci. **115**, 8131 (2018), arXiv:1709.00481.
- [58] K. Chakraborty and B. R. Majhi, Phys. Rev. D **100**, 045004 (2019), arXiv:1905.10554.
- [59] S. Dalui and B. R. Majhi, Phys. Rev. D **102**, 124047 (2020), arXiv:2007.14312.
- [60] S. W. Hawking, Comm. Math. Phys. **43**, 199 (1975).
- [61] W. Unruh, Phys. Rev. D **14**, 870 (1976).
- [62] W. G. Unruh and R. M. Wald, Phys. Rev. D **29**, 1047 (1984).
- [63] S. Hawking and W. Israel, *General Relativity: an Einstein Centenary Survey* (2010).
- [64] K. Zyczkowski, P. Horodecki, A. Sanpera, and M. Lewenstein, Phys. Rev. A **58**, 883 (1998), arXiv:quant-ph/9804024.
- [65] G. Vidal and R. F. Werner, Phys. Rev. A **65**, 032314 (2002), arXiv:quant-ph/0102117.
- [66] J. Eisert and M. B. Plenio, J. Mod. Opt. **46**, 145 (1999), arXiv:quant-ph/9807034.
- [67] I. Devetak and A. Winter, Proceedings of the Royal Society A: Mathematical, Physical and Engineering Sciences **461**, 207 (2005), ISSN 1471-2946.
- [68] C. H. Bennett, D. P. DiVincenzo, J. A. Smolin, and W. K. Wootters, Phys. Rev. A **54**, 3824 (1996), arXiv:quant-ph/9604024.
- [69] S. Hill and W. K. Wootters, Phys. Rev. Lett. **78**, 5022 (1997), arXiv:quant-ph/9703041.
- [70] W. K. Wootters, Phys. Rev. Lett. **80**, 2245 (1998), arXiv:quant-ph/9709029.
- [71] P. Simidzija and E. Martín-Martínez, Phys. Rev. D **98**, 085007 (2018), arXiv:1809.05547.
- [72] D. Grumiller, W. Kummer, and D. V. Vassilevich, Phys. Rept. **369**, 327 (2002), hep-th/0204253.
- [73] B. A. Juárez-Aubry and J. Louko, JHEP **05**, 140 (2018), arXiv:1804.01228.
- [74] L. Hodgkinson, *Particle detectors in curved spacetime quantum field theory* (2013), arXiv:1309.7281.
- [75] E. Martín-Martínez, Phys. Rev. D **92**, 104019 (2015), arXiv:1509.07864.
- [76] E. Tjoa and E. Martín-Martínez, Phys. Rev. D **104**, 125005 (2021), arXiv:2109.11561.
- [77] E. Tjoa and R. B. Mann, JHEP **03**, 014 (2022), arXiv:2202.04084.